Experimental Implementation of a Fiber Noise Cancellation System for Slow Light Laser Locking

Alexander Bengtsson
Supervisor: Lars Rippe

Thesis submitted for the degree of
Master's in Engineering Physics
Project duration: 20 weeks
2017

LUND UNIVERSITY

Atomic Physics Division
Faculty of Engineering, LTH

Abstract

An electromagnetic wave propagating through an optical fiber is sensitive to external disturbances, such as mechanical vibrations and temperature and pressure fluctuations, which add phase noise onto the wave. For high-precision frequency-based applications this phase noise has to be removed. By partially reflecting light from the remote end of the fiber back through the fiber, and comparing it to light that has not passed through the fiber, their beat note can be phase locked to a stable reference, using an acousto-optic modulator for phase noise compensation. This effectively cancels the phase noise at the remote end of the fiber. In this project, two such fiber noise cancellation systems have been successfully assembled. The fiber noise cancellation systems will be used for laser locking to a slow light crystal cavity. Using spectral hole burning, a very low group velocity can be obtained in rare-earth-ion-doped crystals. By depositing mirrors on such a crystal, it could act as a reference cavity with a very long effective length, but without the increased difficulty of isolating the cavity from mechanical vibrations associated with a physically long cavity. By locking a laser to a slow light crystal cavity, an improved stability could potentially be achieved. A possible setup for slow light crystal cavity laser locking experiments, where the fiber noise cancellation systems have been integrated, is also presented in this thesis.

Populärvetenskaplig Sammanfattning

Atomur som är baserade på en optisk frekvens är under utveckling. Dessa optiska klockor är i dagsläget så exakta att om de startades vid big bang, så skulle de bara visa en sekund fel idag. Nästa generations kommunikation- och navigeringssystem kommer att dra nytta av noggrannare tidsmätning. I detta examensarbete behandlas två saker som är viktiga för den fortsatta utvecklingen av optiska klockor: laserstabilisering och eliminering av fasbrus i optiska fiber.

Optiska klockor tar för tillfället upp hela labb och är alltså inte lätta att transportera. Det behövs därför ett sätt att noggrant kunna jämföra klockorna över långa avstånd. Detta kommer troligtvis göras med ett nätverk av optiska fiber. När laserljus färdas genom ett optiskt fiber påverkas det av yttre störningar som vibrationer och förändringar i temperatur och tryck, vilket får längden på fibern att ändras. Detta leder till att ljuset blir brusigt, och ljus som var väldigt enfärgat innan fibern, kommer då bestå av ett bredare spektrum av färger efter fibern. För applikationer som till exempel optiska klockor, där det är önskvärt att kunna överföra väldigt enfärgat ljus med optiska fiber, så behövs detta fiberbrus kompenseras bort. En metod för att göra detta, är att man skickar tillbaka en liten del av ljuset som har färdats genom fibern, och jämför det med ljus direkt från lasern. På detta sätt kan man mäta hur mycket brus som fibern adderar till laserljuset. Det är då möjligt att kompensera för bruset redan innan fibern, så att ljuset ut ur fibern blir brusfritt. I detta examensarbete har två system som gör just detta byggts. Dessa systemen kommer inte att användas för att jämföra klockor, utan för framtida experiment om laserstabilisering till en långsamtljus-kavitet, där det också är viktigt att kunna transportera brusfritt ljus i optiska fiber.

I optiska klockor jämför man frekvensen på en laser med oscillationsfrekvensen för en specifik atom. Genom att hålla laserns frekvens så nära atomens frekvens som möjligt och sedan räkna svängingar för laserljuset, så kan tid mätas. Detta kan jämföras med att räkna svängningarna för en pendel. En laser som konstant ger samma frekvens är därför viktig för optiska klockor. För många lasertyper är det möjligt att kontrollera frekvensen på laserljuset med en elektrisk signal. Genom att mäta frekvensen, kan alltså en lämplig kontrollsignal skickas till lasern, så att ljuset ut från den så nära som möjligt håller sig på samma frekvens. Denna frekvensmätning är ofta gjord med en optisk kavitet, vilket är två speglar som är noggrant riktade mot varandra. Ljus som skickas mot kaviteten kommer antingen att reflekteras tillbaka samma väg som det kom ifrån, eller passera genom kavitet. Om ljuset reflekteras eller passerar beror väldigt starkt på ljusets frekvens, och detta kan då användas för att mäta frekvensen. För att så noggrant som möjligt kunna mäta ljusets frekvens, är det viktigt att längden på kaviteten, alltså avståndet mellan de två speglarna inte ändras. För om längden på kaviteten ändras, så ändras också frekvenserna där ljuset tillåts passera kaviteten. I teorin är det fördelaktigt med en så lång kavitet som möjligt. I praktiken visar det sig dock vara svårt att isolera en lång kavitet från mekaniska vibrationer som får kavitetens längd att ändras. Långsamt ljus skulle kunna användas för att undgå detta problem. I kristaller där joner av så kallade sällsynta jordartsmetaller har tillsats vid tillverkningen, är det möjligt att minska ljushastigheten avsevärt. Genom att sätta speglar på ändarna av en sådan kristall, så har nu en långsamtljus-kavitet skapats. Den kraftigt sänkta ljushastigheten får en sådan kavitet att bete sig som en lång kavitet, fast utan den extra svårigheten med att otroligt väl behöva isolera kaviteten från mekaniska vibrationer, som tillkommer för en fysiskt lång kavitet. I detta examensarbete presenteras en möjlig uppställning för laserstabilisering till en långsamtljus-kavitet.

Abbreviations

AOM - Acousto-Optic Modulator

BS - Beam Splitter

EOM - Electro-Optic Modulator

FM - Frequency Modulation

PD - Photodetector

PDH - Pound-Drever-Hall

PI - Proportional-Integral

Pr^{3+} - Triply ionized praseodymium

RF - Radio Frequency

VCO - Voltage Controlled Oscillator

Contents

1 Introduction

The atomic clocks used as frequency standards today are based on cesium, and the second is defined as the duration of 9 192 631 770 cycles of the radiation that is resonant with a certain microwave transition in cesium 133 [1]. By increasing the operational frequency of an atomic clock from the microwave to the optical frequency range, the second can be divided into smaller intervals, making it possible to build even more accurate clocks. Optical clocks have reached an uncertainty and instability at the 10^{-18} level [2]. This is astonishingly accurate considering that such a clock would only lose or gain one second over the age of the universe. Optical clocks can be used to investigate if the fundamental constants change over time, verify predictions of quantum electrodynamics, and for very precise tests of Einstein's general theory of relativity. Improved timekeeping may also be beneficial for other applications such as satellite navigation systems and very long base-line interferometry [3]. To realize these clocks, extremely stable lasers are crucial, as they serve as the flywheel oscillator used to probe the atomic resonance. Laser stabilization therefore plays an essential role in the development of optical clocks. Other research areas with high demands on laser stability are gravitational wave detection and quantum information research [4].

The most precise optical clocks and frequency standards are very bulky and not easily transportable. Long distance frequency transfer and remote comparison of atomic clocks are therefore commonly done via satellite links, with a fractional instability of 10^{-15} at one day integration time [5]. To harness the full potential of optical clocks, other techniques for frequency transfer have been developed. One likely way frequency standards will be distributed over long distances in the future, is via optical fiber networks. When light propagates through a fiber, phase noise will be induced by mechanical vibrations, as well as fluctuations in temperature and pressure. But this can be compensated for using fiber noise cancellation methods. A frequency-stabilized laser has been transmitted with a relative frequency uncertainty below $1 \cdot 10^{-19}$ over a 146 km long fiber [6]. Even for shorter fibers connecting different parts of a setup in a laser laboratory, fiber noise can be detrimental and needs to be compensated for. A 25 meter long fiber has been shown to broaden the spectrum of a laser towards the kHz domain [7].

1.1 Background & Aim of this Project

The Quantum Information Group at Lund University carries out research regarding quantum computing and quantum memories, using rare-earth-ion-doped crystals, e.g., Pr^{3+}:Y_2SiO_5 (triply ionized praseodymium doped yttrium silicate) and Eu^{3+}:Y_2SiO_5 (triply ionized europium doped yttrium silicate). A project on laser stabilization using these crystals has also recently been started.

The frequency stability of a laser can be improved by locking the laser to a resonance peak of an external reference cavity. The stability of the locked laser is limited by the stability of the reference cavity, and should increase with the length of the cavity. But it is very hard to isolate a long cavity from mechanical vibrations, making it impractical to construct such a cavity. It may be possible to improve stability with slow light effects. Using spectral hole burning, slow light can be generated in rare-earth-ion-doped crystals. Since there will be a rapid change in the refractive index over the spectral hole, a high group index and thus a low group velocity will be obtained for light with a frequency inside the hole. A slow light crystal cavity will therefore have a long effective length, but without the increased difficulty of isolating the cavity from mechanical vibrations associated with a physically longer cavity. This could lead to an improved stability, and therefore motivates why one would attempt to lock a laser to a slow light cavity.

The group's present laboratory setup is based on a modified Coherent 699-21 dye laser, pumped by an Nd:YVO_4 laser (Coherent Verdi V6). The dye laser is tunable from about 570 nm to 635 nm with Rhodamine 6G, and can thus provide light at the desired wavelengths of 606 nm or 580 nm, depending on if experiments on praseodymium or europium are conducted, respectively. The laser is locked to an external high finesse reference cavity with the Pound-Drever-Hall (PDH) technique to provide high frequency stability, and a linewidth on the order of 10 Hz. Two acousto-optic modulators (AOMs) are used to precisely control the amplitude and phase of the laser light going to the experiment. An arbitrary waveform generator (AWG), controlled from a computer drives the AOMs. For such a setup, it becomes important to compensate for the kHz broadening of the laser spectrum by the fibers connecting different parts of the setup.

My first task was to assemble two fiber noise cancellation systems in the setup. In Figure 1.1, a simplified overview of the laboratory setup is shown and the two fibers that needed stabilization are marked. The locking cavity for the PDH stabilization is located on a vibration isolation platform on the optical table. An optical fiber is needed to guide the light up to this platform. This is the first fiber that was stabilized. The plan is that this fiber noise cancellation system is going to be operative at all times when the laser is on, to provide a more stable signal to the PDH locking. The second fiber that needed stabilization is the one going from the laser table, to the table with the cryostat where the experiments are carried out. This fiber noise cancellation system will be important for the experiments on laser locking to a slow light cavity, where a stable and narrow-linewidth signal will be desirable when attempting to lock the laser to a cavity resonance. Future experiments on europium will also benefit from stabilizing this fiber. Europium has a homogeneous linewidth of 122 Hz [8]. For quantum computing experiments, the ions used as qubits has to be efficiently controlled by the laser. To do this, it is important that the laser linewidth is less than the homogeneous linewidth of the ions. There has been work done on fiber noise cancellation in the group by former master's students. A fiber noise cancellation system was conceptually designed by Adam Wiman [1]. Anders Rönnholm realized it with real components and tested the system, but he used a mirror attached to a piezo crystal to simulate the fiber noise instead of an actual fiber [9]. The fiber noise cancellation systems I will assemble, will largely be based on their work.

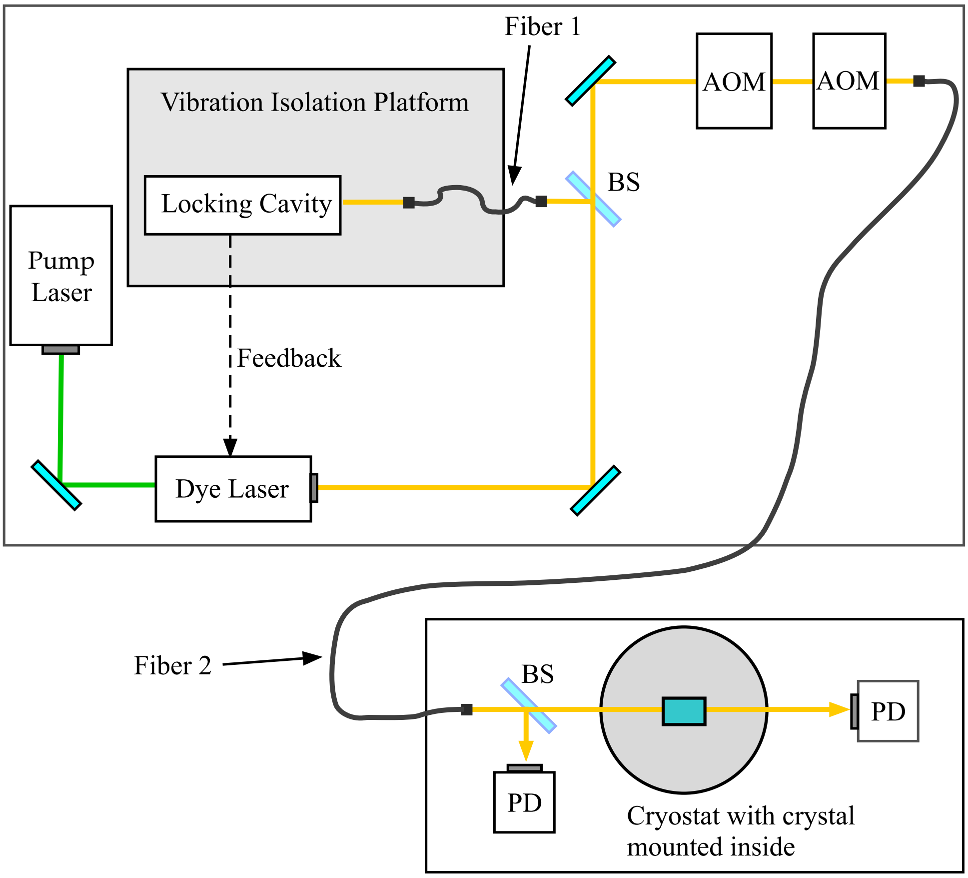

Figure 1.1: A simplified overview of the setup in the laboratory. Two fiber noise cancellation systems were assembled to compensate for the phase noise induced by the two marked fibers.

My second task was to investigate how to lock a laser to a slow light cavity, and assemble an experimental setup. Laser locking experiments were then planned. This has previously been attempted by the master's thesis student Theodor Strömberg [4] and his work lays the foundation for the locking experiments. Successfully locking a laser to a slow light cavity would contribute to the area of laser frequency stabilization, since this has not previously been done.

1.2 Outline of the Thesis

This thesis is divided into eight sections. The introduction is meant to give the reader a brief background to why laser stabilization and fiber noise cancellation is important in general, and also what the aim of this project is. Section 2 provides information on the fiber noise cancellation method used in this project. Section 3 discusses theoretical aspects behind laser locking to a slow light cavity. The initial testing of the fiber noise cancellation system is given in Section 4. In Section 5 and 6 the assembling and evaluation of the two fiber noise cancellation systems are described. The laser locking setup is described in Section 7, and Section 8 provides a summary and outlook.

2 Fiber Phase Noise Cancellation

Optical fibers provide a convenient and efficient way to transfer optical signals from one location to another. Both for long distance frequency transfer over hundreds of kilometers and for shorter distances inside a laboratory. They are also great for avoiding alignment instabilities in a setup. Light propagating through a fiber will be affected by different mechanisms. The light will be attenuated, i.e. a reduction in the light intensity with propagation distance in the fiber, primarily from scattering and absorption. A temporal broadening of the signal will occur from different types of dispersion, such as chromatic dispersion and modal dispersion. The fiber is also sensitive to external disturbances, which induce fiber phase noise to the signal propagating through the fiber.

2.1 Fiber Phase Noise

Phase noise is the rapid and random fluctuations in the phase of a signal. An ideal signal can be described as a pure sine wave, and would then be represented as a single spectral line in the frequency domain. There are however always unwanted fluctuations in the phase of a signal. This leads to a broadening of the signal in the frequency domain, which is illustrated in Figure 2.1.

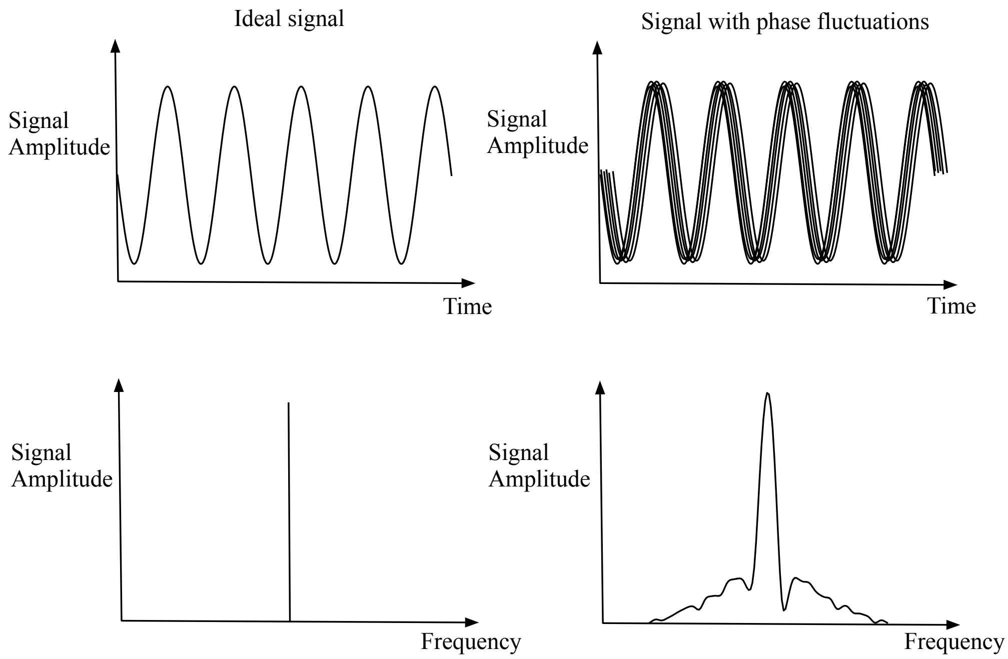

Figure 2.1: An ideal signal is represented by a single spectral line in the frequency domain (left). Phase fluctuations cause a broadening of the signal in the frequency domain (right).

If an electromagnetic wave with frequency ν_0, and zero frequency noise is propagated along an optical fiber with refractive index n and length L, its phase fluctuations in radians, $\delta\varphi$, can be described according to

$$\delta\varphi = \frac{2\pi\nu_0}{c}(L\delta n + \delta L n), \tag{2.1}$$

where c is the speed of light in vacuum. Random changes in the optical path length of a fiber over time thus add phase noise to the electromagnetic wave propagating through the fiber, thereby degrading its stability. The optical path length changes if either the refractive index or the physical length of the fiber changes. A fiber is therefore sensitive to fluctuations in temperature, since both the refractive index and the physical length are temperature dependent. Phase fluctuations in the transmitted electromagnetic wave can also originate from acoustic pressure waves or mechanical vibrations, which induce stresses and strains inside the fiber, altering the length and refractive index of the fiber. If the phase noise $\varphi(t)$ is known, the instantaneous frequency in Hz, $\nu(t)$, is given by

$$\nu(t) = \nu_0 + \frac{1}{2\pi}\frac{d\varphi(t)}{dt}, \tag{2.2}$$

where the last term represents the frequency noise.

2.2 Compensating for Fiber Induced Phase Noise

Different approaches exist to compensate for fluctuations in the optical path length of a fiber. Piezo-actuated fiber-stretchers or thermally controlled spools of fiber can be used [10]. The fiber noise can also be compensated for with an acousto-optic modulator (AOM), that pre-modulates the light with a negative image of the fiber noise, making the light at the far end of the fiber noise free. This is the approach used for both fiber noise cancellation systems built during this project, and it is also described in [1, 7, 9]. A disadvantages with using an AOM is that the AOM reduces the transmitted power slightly, but an efficiency of 80 % is readily achievable. Before the fiber noise cancellation scheme is described, some general theory about some of the components and techniques used in the scheme is given.

2.2.1 Acousto-Optic Modulator

The AOM is a useful component for many photonics applications, and can be used to modulate the frequency, intensity and direction of a laser beam. In an AOM, a piezoelectric transducer attached to a crystal is driven by a radio frequency (RF) signal. This generates an acoustic sound wave propagating through the crystal. When the acoustic wave propagates through the crystal, regions were the crystal is compressed and rarefied are generated. This leads to a periodically varying refractive index with the same period as the acoustic wave, which acts as a diffraction grating, splitting the incident light into several diffraction orders, see Figure 2.2. Because the grating is propagating through the crystal, the diffracted light will be Doppler shifted. This frequency shift, Δf, is given by

$$\Delta f = mF, \tag{2.3}$$

where F is the frequency of the acoustic wave and m is the diffraction order. The frequency and phase of the laser input can therefore be modulated by modulating the frequency of the acoustic wave. The separation angle between the zero order and first order beams in radians θ_{sep}, depends on the wavelength of the light λ, the frequency of the acoustic wave F, and the acoustic velocity in the crystal V as

$$\theta_{sep} \approx \frac{\lambda F}{V}. \tag{2.4}$$

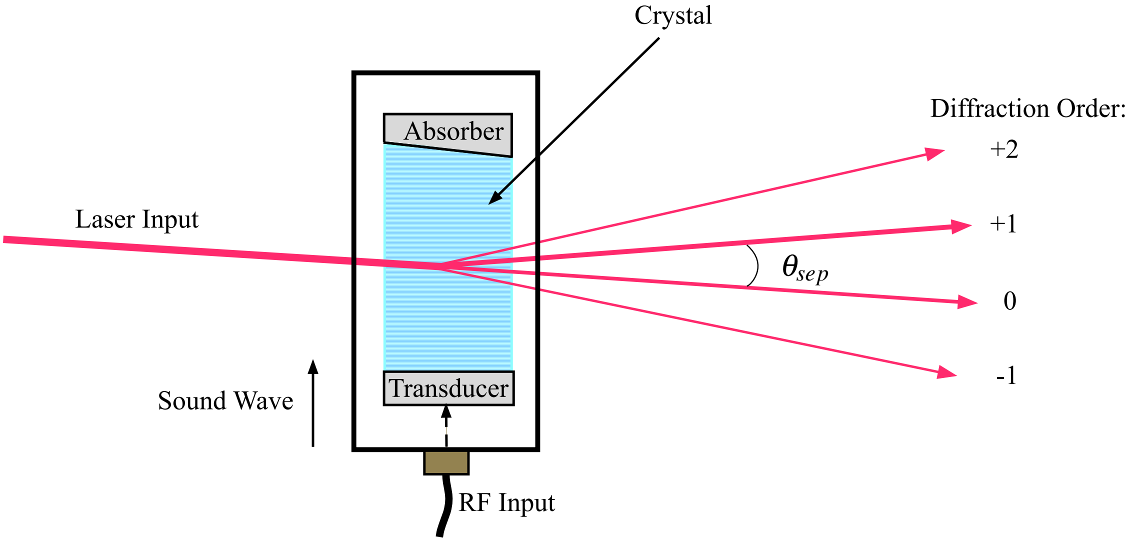

Figure 2.2: An illustration of an AOM. An RF signal is sent to a piezoelectric transducer which generates an acoustic wave propagating through the crystal. The laser input is divided into several diffraction orders. An absorber prevents back reflections from interacting with the light. The diffraction angles in this figure are exaggerated and actually smaller in reality.

2.2.2 The PI Controller

The output of a dynamical system can be modified through feedback. In Figure 2.3, a block diagram of a negative feedback control system is shown. By measuring the difference between the system output and a desired reference, an error signal $e(t)$ is obtained. From the error signal, the controller calculates a control signal $u(t)$ such that the system output as closely as possible follows the reference.

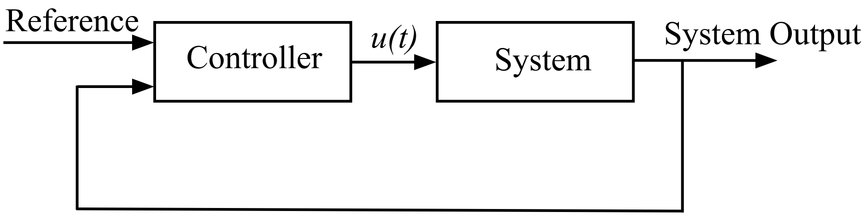

Figure 2.3: A negative feedback system.

The proportional-integral (PI) controller is a commonly used controller. The control signal for this controller is calculated based on two terms, the proportional term and the integral term, according to

$$u(t) = \underbrace{K_p e(t)}_{\text{P-term}} + \underbrace{\frac{K_p}{T_i} \int e(t) dt}_{\text{I-term}}, \tag{2.5}$$

where K_p is the proportional gain and T_i is the time constant [11], which are the two tuning parameters of the controller.

Tuning a PI Controller

The Ziegler-Nichols method can be used to tune a PI controller. First, the I-part of the controller is turned off and the proportional gain is set to zero. The controller is then put into automatic mode and the proportional gain is increased until oscillations in the signals of the control system are observed. This is the critical gain value K_{p0}. The period of the oscillations is the critical period T_0. The proportional gain of the PI controller is then given by

$$K_p = 0.45K_{p0}, \tag{2.6}$$

and the time constant, T_i, is calculated according to [11]

$$T_i = \frac{T_0}{1.2}, \tag{2.7}$$

where the corner frequency, f_{PI}, is

$$f_{PI} = \frac{1}{2\pi T_i}. \tag{2.8}$$

2.2.3 Optical Heterodyne Detection

Photodetectors do not have a fast enough response time to directly measure the frequency of optical signals. Optical frequency measurements can however by done by down-converting the signal to the RF regime. If two laser beams with a small frequency difference $\Delta\nu$ are overlapped on beam splitter and directed to a photodetector, a beating at the optical difference frequency can be detected as a result of the interference between the two beams. The mean photocurrent from the photodetector, $\bar{\imath}$, is given by

$$\bar{\imath} = \bar{\imath}_1 + \bar{\imath}_2 + 2\sqrt{\bar{\imath}_1\bar{\imath}_2}cos(2\pi\Delta\nu t + \Delta\phi), \tag{2.9}$$

where $\bar{\imath}_1$ and $\bar{\imath}_2$ are the photocurrents generated by the two beams individually, and $\Delta\phi$ is the phase difference between the two beams [12]. By AC coupling the photodetector, the photocurrent can be written as

$$\bar{\imath} \propto \sqrt{\bar{\imath}_1\bar{\imath}_2}cos(2\pi\Delta\nu t + \Delta\phi). \tag{2.10}$$

2.2.4 Phased Locked Loop

A phase locked loop is circuit based on comparing the phase of two signals, and then constantly adjust to hold (lock) these signals in phase. A block diagram of a phased locked loop is shown in Figure 2.4. The three basic components are a phase detector, a loop filter, and a voltage controlled oscillator (VCO). The phase detector compares the phase of the reference and the VCO signal, and outputs a voltage depending on the phase difference between the signals. By applying appropriate filtering on the phase detector output, the VCO can be modulated to output a signal that is locked in phase with the reference signal.

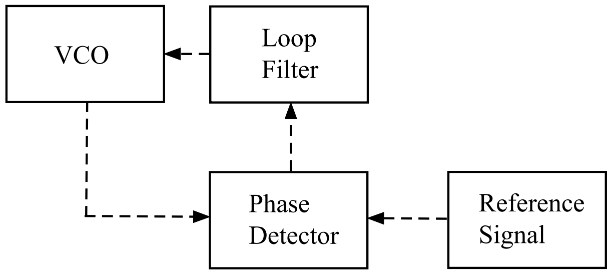

Figure 2.4: A block diagram of a phase locked loop.

2.2.5 The Cancellation Scheme

The basic fiber noise cancellation scheme is shown in Figure 2.5. Let the light from the laser be denoted $E = cos(\omega_l t)$, where ω_l is the laser frequency. The light is sent through an AOM which divides it into several diffraction orders, but with the AOM set such that most of the power is in the +1st and 0th order beams. The +1st order beam is frequency shifted $\omega_{ref}/2$ by the AOM, which is half the reference oscillator frequency. The AOM also adds a phase correction θ_c. After passing the AOM the +1st order beam can thus be described by

$$E_{1st} = cos\left[(\omega_l + \frac{\omega_{ref}}{2})t + \theta_c\right]. \tag{2.11}$$

The +1st order beam is coupled into the optical fiber. A beam splitter at the remote end of the fiber reflects some of the light back through the fiber, and transmits the rest for experimental use. Fiber phase noise, θ_f, will be induced by each passage through the fiber, and it can be assumed that the phase noise of two passages is twice that of a single passage [7]. Hence, a phase shift of $2\theta_f$ is added to the laser beam by the fiber. The retro-reflected +1st order beam then passes the AOM again where it gets frequency shifted once more by $\omega_{ref}/2$, and a phase correction θ_c is added. After passing the AOM the second time, the +1st order beam can therefore be described by

$$E_{1st} = cos\left[(\omega_l + \omega_{ref})t + 2(\theta_c + \theta_f)\right]. \tag{2.12}$$

The 0th order beam is reflected back through the AOM by a mirror and is not affected by any of the two passes through the AOM, and can thus be described by

$$E_{0th} = cos(\omega_l t). \tag{2.13}$$

Both beams are picked off by a beam splitter and overlapped on a photodetector, where a beating signal at the difference frequency containing information on twice the fiber phase noise is detected as

$$V_{beat} = cos\left[\omega_{ref} t + 2(\theta_c + \theta_f)\right]. \tag{2.14}$$

This beating signal is sent to a phase detector, and so is a reference signal from a stable reference oscillator with frequency ω_{ref}, and phase fluctuations that can be considered zero compared to the phase fluctuations of the laser. The reference signal is given by

$$V_{ref} = cos(\omega_{ref} t). \tag{2.15}$$

The phase detector outputs a voltage depending on the phase difference between the two input signals. The PI controller takes this voltage and outputs a control signal to the VCO, which in turn prescribes the phase correction θ_c to the AOM, in an attempt to minimize the phase difference between the two signals. In practice this phase correction is done by slightly adjusting the driving frequency to the AOM. The system constantly adjusts to hold the phase difference at zero, i.e. $2(\theta_c + \theta_f) = 0$, and the signals are thereby phase locked. The light at the remote end of the fiber can then be described by

$$E_{rem} = cos\left[(\omega_l + \frac{\omega_{ref}}{2})t + \theta_c + \theta_f\right] = cos\left[(\omega_l + \frac{\omega_{ref}}{2})t\right]. \tag{2.16}$$

The light at the remote end of the fiber will shifted by $\omega_{ref}/2$, but the the control system compensates for the fiber phase noise preserving the stability.

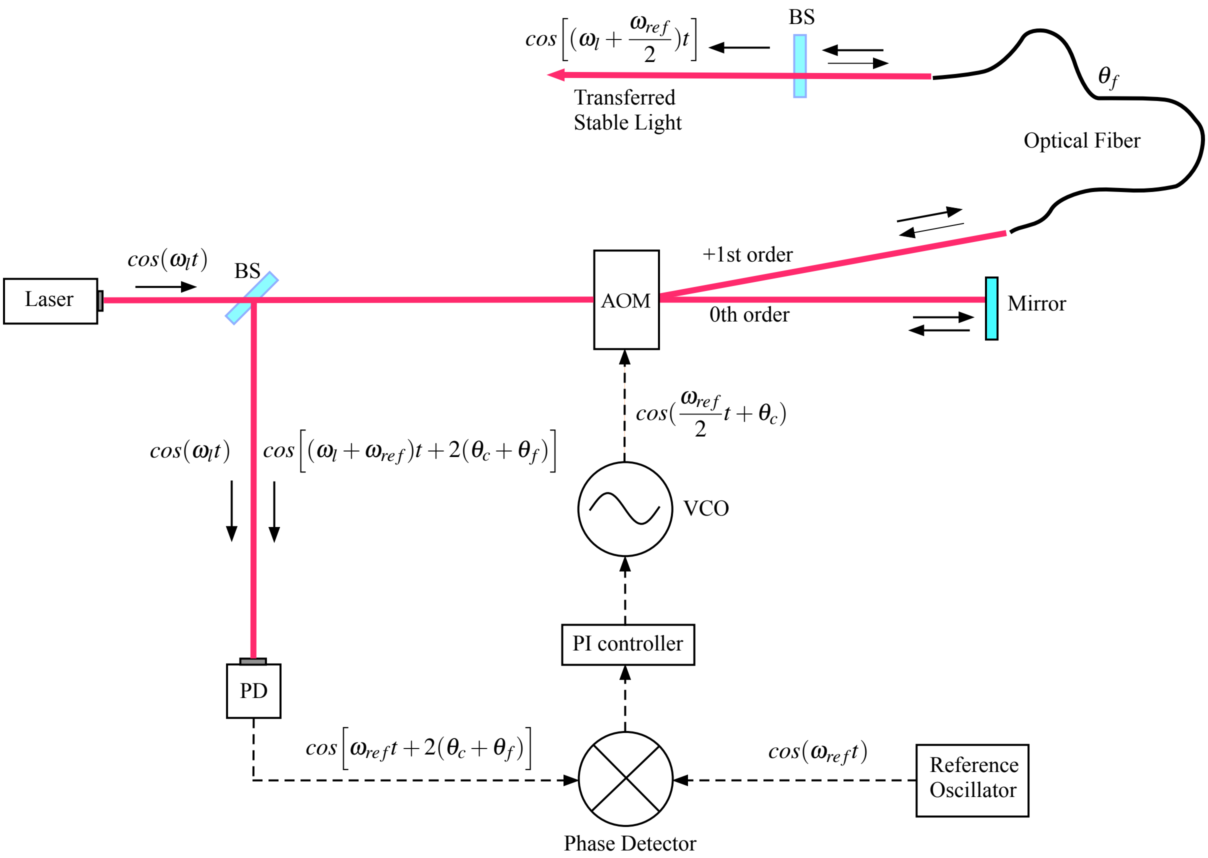

Figure 2.5: The fiber noise cancellation scheme.

For this fiber noise cancellation method to work efficiently, the system has to be able to compensate for phase noise fast enough. Limiting factors can be the finite speed of light, the response time of electronic components and how fast the AOM can be frequency modulated [9]. Fortunately, mechanical vibrations and fluctuations in temperature and pressure are rather slow processes. As an example, consider an acoustic pressure wave with frequency 2 kHz. This corresponds to noise with a period of 500 μs. For a fiber with length $L = 50$ m and refractive index $n = 1.5$, a laser beam propagates back and forth through the fiber in a time, τ, given by

$$\tau = \frac{1.5 \cdot 100}{3 \cdot 10^8} = 0.5\ \mu\text{s}. \tag{2.17}$$

The beam thus propagates back and forth through the fiber in a time interval three orders of magnitude shorter than the noise period. This means that the optical path length does not change significantly during the two passages through the fiber, and also that the phase noise of two passages is twice that of a single passage. Since electrical signals travel at a speed comparable to the speed of light, signal delay in cables does not effect the performance of the system. The component that limits the regulating speed in the setup that is going to be assembled in this project, is the VCO modulating the AOM [9]. The AOM has to have a frequency modulation (FM) bandwidth larger than the phase noise bandwidth [13].

3 Laser Stabilization

3.1 Pound-Drever-Hall Laser Stabilization

Many lasers are electrically tunable. By measuring the laser frequency and applying appropriate filtering, a control signal can be sent to the tuning port of the laser to suppress frequency fluctuations. The PDH technique is a common way of improving the frequency stability of a laser, where the laser is stabilized to an external frequency reference such as a cavity, an absorption line, or a spectral hole [14].

The reflected intensity from an optical cavity as a function of laser frequency is show in Figure 3.1. When the incident light matches very specific frequencies, the reflection from the cavity vanishes due to destructive interference between the reflection from the first cavity mirror and the cavity leakage field. The resonant frequencies occur at an integer times the cavity's free spectral range, $\Delta\nu_{fsr} \equiv c/2L$, where L is the length of the cavity. The full width at half-maximum of a resonance is called the linewidth. In the PDH technique, the laser is locked to one of these resonances. Unfortunately, the reflected intensity is symmetric around the resonance. This means that it is not possible to tell if an increase in the reflected intensity originates from an increase or decrease in laser frequency. The phase of the reflected field is however asymmetric around resonance, see Figure 3.1.

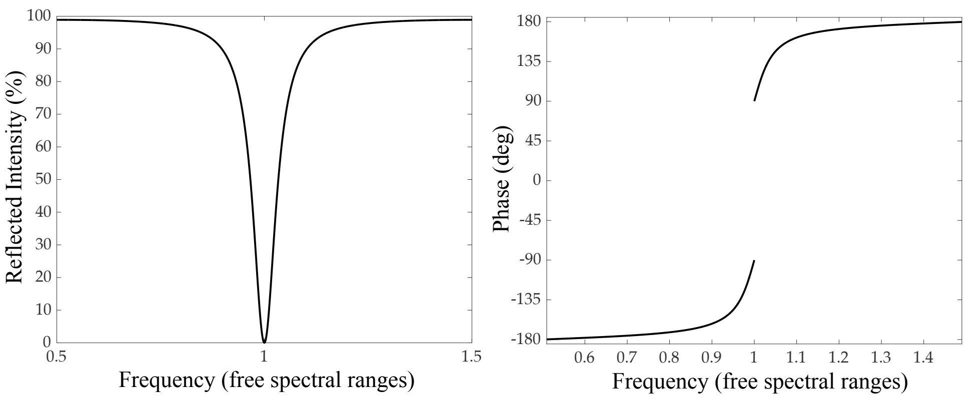

Figure 3.1: Reflected intensity (Left) and phase (right) from an optical cavity with a finesse of 30.

There is no electronics available that directly measures the phase of an electromagnetic field. It is however possible to obtain phase information by comparing one electromagnetic field to another. In Figure 3.2, a basic PDH locking setup is illustrated. The PDH technique uses an electro-optic modulator (EOM) to phase modulate the light before the reference cavity, with a modulation frequency Ω. The magnitude of an electromagnetic field, $E(t)$, with frequency ω and amplitude E_0 can be written as

$$E(t) = E_0 e^{i\omega t}. \tag{3.1}$$

The phase modulated field, $E_{mod}(t)$ can then be described by [15]

$$\begin{aligned} E_{mod}(t) &= E_0 e^{i(\omega t + \beta sin\Omega t)} \\ &\approx \underbrace{J_0(\beta)E_0 e^{i\omega t}}_{\text{Carrier}} + \underbrace{J_1(\beta)E_0 e^{i(\omega+\Omega)t}}_{\text{Sideband}} - \underbrace{J_1(\beta)E_0 e^{i(\omega-\Omega)t}}_{\text{Sideband}}. \end{aligned} \tag{3.2}$$

Here the expression has been expanded using Bessel functions $(J_0(\beta),(J_1(\beta))$. Higher order terms can be neglected if a modulation depth $\beta < 1$ is chosen, because then most of the power is in the carrier and first order sidebands [15]. From Eq. 3.2 it can be seen that by phase modulating the light, sidebands at frequencies $\omega \pm \Omega$ have been generated. The sidebands have a definite phase relationship to the carrier [15]. By choosing the modulation frequency much larger than the cavity linewidth, the sidebands will be completely reflected, while the carrier will couple into the cavity, and only be reflected if the laser drifts off resonance. If the reflection from the cavity is measured on a photodetector, beating signals at Ω and 2Ω will be observed, corresponding to the interference between sideband-carrier and sideband-sideband, respectively. The Ω-term is the signal of interest, since the phase of this signal contains information on the carrier phase, which can be used to deduce which side of resonance the carrier is on. Phase sensitive detection can be done with a mixer and a low-pass filter. The signal from the photodetector is mixed with a reference signal from the oscillator at the same frequency as the signal sent to the EOM. The phase shifter can be used to compensate for unequal delays in the two signal paths. When the photodetector measures a signal oscillating at Ω, the output of the mixer will contain a DC-signal, since a mixer outputs the product of its inputs, which is signals oscillating at the the sum and difference frequencies. This DC-signal can be filtered out using a low-pass filter, and will be a monotonic slope close to resonance with a zero crossing at the resonance. With appropriate feedback from the PID controller to the laser, the system can now be locked to this zero crossing.

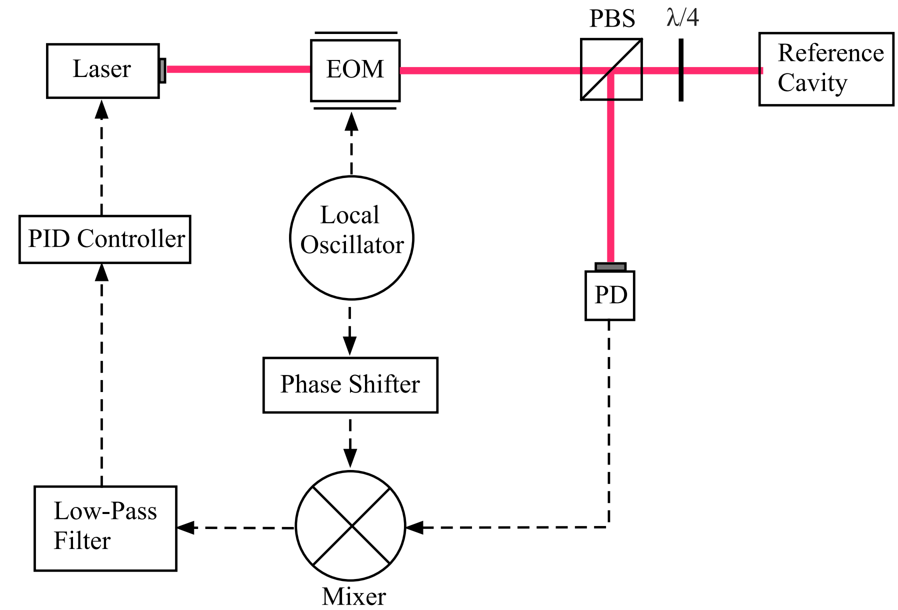

Figure 3.2: A basic PDH locking setup. An optical isolator consisting of a polarizing beam splitter (PBS) and a $\lambda/4$-plate is used to pick off the reflection from the reference cavity and direct it to the photodetector (PD).

3.2 Slow Light Cavity

The phase velocity, v_p, is the propagation speed of a single frequency component of light, and is given by

$$v_p = \frac{c}{n(\nu)}, \tag{3.3}$$

where $n(\nu)$ is the refractive index and c is the speed of light in vacuum. A medium with a refractive index that depends on the frequency ν, is called a dispersive medium. In such a medium, monochromatic light waves with different frequencies do not propagate with the same phase velocity.

A pulse of light can be seen as the sum of several monochromatic light waves with different frequencies, amplitudes and phases. When a pulse of light propagates through a dispersive medium, it is therefore the sum of many frequency components propagating at different phase velocities that characterize how the pulse propagates. This means that even if the different frequency components of a pulse propagate at a speed comparable to c, the pulse may not. The velocity for a pulse, v_g, called the group velocity therefore has to be introduced, and is given by [4]

$$v_g = \frac{c}{n + \nu \frac{dn}{d\nu}}. \tag{3.4}$$

From the group velocity, the group index n_g can be calculated as

$$n_g = \frac{c}{v_g}. \tag{3.5}$$

From Eq.3.4 it can be seen that a very strong dispersion slope, $\frac{dn}{d\nu}$, would lead to a greatly reduced group velocity. Strong dispersion can be achieved in rare-earth-ion-doped crystals using a technique known as spectral hole burning. By depositing mirrors on the crystal sides, a slow light cavity can be created.

3.2.1 Spectral Hole Burning

If an yttrium silicate crystal is doped with praseodymium ions, strains will be induced in the crystal, since the ions are not completely compatible with the crystal structure. The strains will vary slightly with location in the crystal, and therefore cause different ions to absorb radiation at slightly different frequencies. An inhomogeneous absorption profile is obtained by adding all the homogeneous absorption profiles of each individual ion, see Figure 3.3.

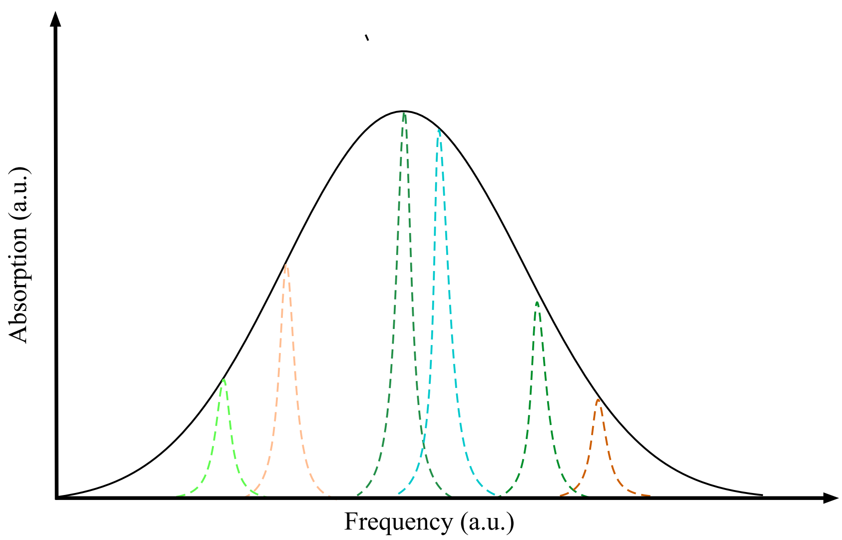

Figure 3.3: The inhomogeneous absorption profile (black envelope), consisting of several homogeneous absorption lines (some of them are illustrated with dashed colored lines).

The hyperfine levels of the $^3H_4 \leftrightarrow {}^1D_2$ transition in praseodymium can be seen in Figure 3.4. By tuning a laser within the inhomogeneous absorption profile a spectral hole can be created. This is a decrease in absorption for the material. If the laser e.g. is tuned to match the $|1/2g\rangle \rightarrow |1/2e\rangle$ transition for a group of ions, the ions will first be excited. They can then decay to any of the three lower states. The ions that decay back to the $|1/2g\rangle$ state can be excited once again by the same laser frequency. If they on the other hand decay to the $|3/2g\rangle$ or $|5/2g\rangle$ states, the ions cannot be excited by the laser anymore. This leads to an emptying of the $|1/2g\rangle$ state and thus a decrease in absorption for the frequency corresponding to the $|1/2g\rangle \rightarrow |1/2e\rangle$ transition, i.e., a spectral hole.

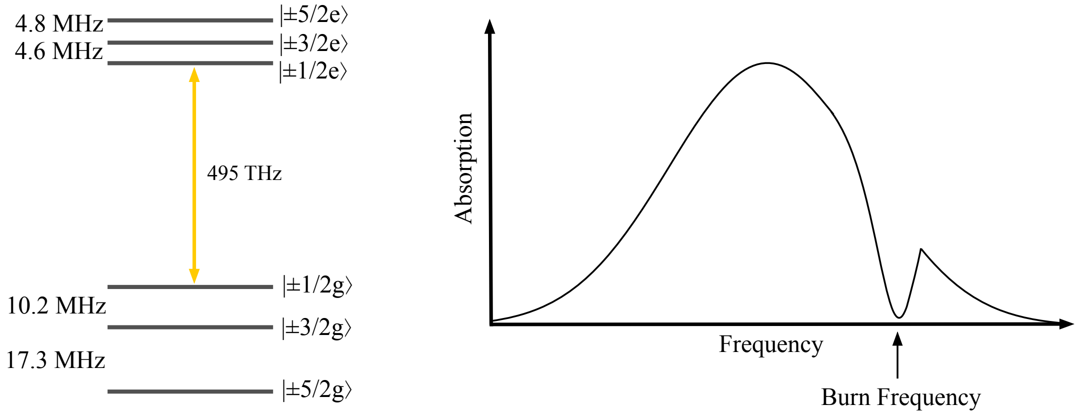

Figure 3.4: The hyperfine levels of the $^3H_4 \leftrightarrow {}^1D_2$ transition in praseodymium (left). By exposing the ions to a laser with a frequency within the inhomogeneous absorption profile, a spectral hole can be created (right).

By employing a sequence of frequency scanning laser pulses, a spectral region within the inhomogeneous absorption profile which is completely emptied of absorbers can be tailored. The maximum width of this spectral region is however limited by the total splitting of the hyperfine levels in the ground and excited state. For praseodymium, this width is 18.1 MHz. By attempting to burn a wider structure, the ions will only be continuously cycled between the different ground states.

3.2.2 Light Propagation Near Spectral Holes

The absorption of a frequency component of a light pulse, has to be linked to compensatory phase shifts amongst the other frequency components of the pulse, or else the theory of electromagnetism would contradict causality [16]. For a medium to be absorptive, it is thus necessary for the medium to also be dispersive, i.e., have a frequency dependent refractive index.

Absorption measurements for optical media are commonplace. For a low dispersion crystal host with refractive index n_0, and embedded resonant ions, the dispersion spectrum can be calculated from the absorption coefficient in m^{-1}, $\alpha(\nu)$, as follows. First the imaginary part of the susceptibility for the embedded resonant ions, $\chi''(\nu)$, can be calculated as [12]

$$\chi''(\nu) \approx -\frac{n_o c}{2\pi\nu}\alpha(\nu). \tag{3.6}$$

It is then possible to obtain the real part of the susceptibility for the resonant ions $\chi'(\nu)$ through one of the Kramer-Kronig relations given by

$$\chi'(\nu) = \frac{2}{\pi}\int_0^\infty \frac{s\chi''(s)}{s^2-\nu^2}ds. \tag{3.7}$$

Finally, the refractive index can be calculated using [12]

$$n(\nu) \approx n_0 + \frac{\chi'(\nu)}{2n_0}. \tag{3.8}$$

In Figure 3.5, the refractive index as a function of frequency for a rectangular spectral hole is shown. Inside the spectral hole, the refractive index is changing rapidly with frequency, which is the desired property to induce slow light. A narrower spectral hole gives a stronger dispersion and a lower group velocity.

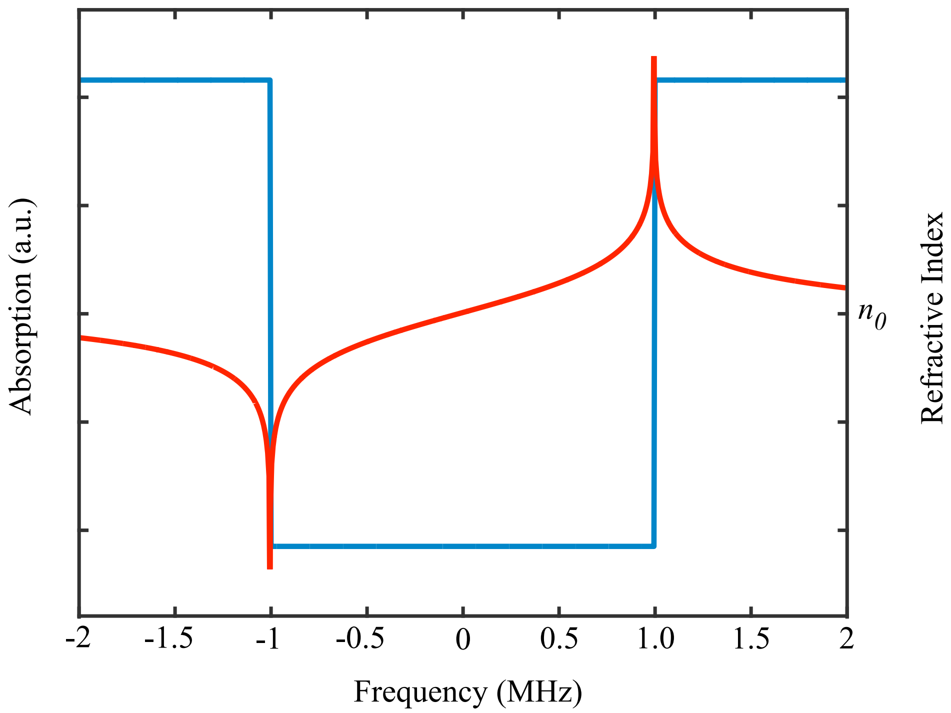

Figure 3.5: An illustration of the dispersion of the refractive index (red line) for a rectangular absorption structure (blue line).

3.2.3 Frequency Stability

The fractional length change of a cavity, $\frac{dL}{L}$, is related to the fractional frequency change of a cavity resonance, $\frac{d\nu}{\nu}$, according to [4]

$$\frac{d\nu}{\nu} = -\frac{dL}{L}\frac{n(\nu)}{n_g}. \tag{3.9}$$

The ultra-stable high finesse cavities typically used as frequency references for laser stabilization, have a cavity length of about 10-20 cm. In theory, a longer cavity should lead to an improved stability. A small change in length for a long cavity, would give a smaller fractional frequency change of a cavity resonance, compared with a short cavity subjected to the same length change. Unfortunately, it is very difficult to isolate a long cavity from mechanical vibrations, and an improved stability is not easily obtained by just building a longer cavity.

In Eq. 3.9, the advantages of using a slow light cavity becomes apparent. The fractional frequency change of a cavity resonance caused by a fractional length change of the cavity will be strongly dampened by the dispersion. For a 6 mm long 0.05% doped Pr^{3+}:Y_2SiO_5 crystal with 95 % reflectivity mirrors, a longitudinal mode spacing of $\approx$ 220 kHz has been demonstrated [17]. In vacuum this correspond to a cavity length of $\approx$ 700 m! The short crystal cavity therefore behaves as a much longer cavity. But at the same time, the difficulty of having to isolate the cavity from mechanical vibrations normally associated with a physically long cavity is avoided.

For slow light crystal cavity locking experiments, it is advantageous to probe the cavity resonance with stable and narrow-linewidth laser light. Having an optical fiber in the setup that induces phase noise, and broadens the spectrum of a narrow-linewidth laser towards the kHz domain, would make it more difficult when attempting to lock a laser to a resonance peak. Because an optical fiber connects the laser table and the table with the crystal cavity in the Quantum Information Group's laboratory, a fiber noise cancellation system is necessary for laser locking experiments.

4 Testing the Fiber Noise Cancellation System

Before the two fiber noise cancellation systems for the dye laser setup were realized, a test system using a HeNe laser was assembled. This was done both to learn how the fiber noise cancellation system works, and to see if all the necessary equipment for the two systems was available and functioning.

Unfortunately the test system never worked as well as I had hoped for. Several problem were encountered. The amplitude of the beating signal between the +1st and 0th order beams on the photodetector changed rapidly over time, by as much as a factor of 4. When the +1st order beam was blocked, a beating signal was surprisingly still measured. Also, the HeNe lasers internal frequency stabilization was not working properly; it was turning on and off. Because the goal of this projects was not to build a fiber noise cancellation system for the HeNe laser, not much time was spent on solving these problems. All the equipment that was intended to be used for the two fiber noise cancellation systems for the dye laser setup did however appear to be working correctly.

4.1 Additional Equipment

The 0th and +1st order beams have to be efficiently separated by a mirror after the AOM. This can advantageously be done using a D-shaped mirror. Two D-shaped mirrors (BBD1-E02) and their associated mirror mount (KM100D) were therefore bought from Thorlabs, one for each fiber noise cancellation system. A 1/2" mirror (BB05-E02), a kinematic mirror mount (KM05/M) and a 45° mount (H45A) for this mirror were also bought from Thorlabs, and will be used to pick off the reflected beams for one of the cancellation systems. The phase detectors are designed to have a 500 Ω load at the output. The PI-controllers have 1 MΩ inputs, and a circuit for matching the impedances is therefore needed. This can be accomplished with the simple circuit shown in Figure 4.1, which also works as a low pass filter with a cutoff frequency of roughly 1 MHz. Five brass housings with SMA connectors in both ends (SMA-KIT-1.5MF) were bought from Digi-Key, and two filters with the circuit shown in Figure 4.1 were built. In Figure 4.2 a photograph of one of the RC filters that was built is shown.

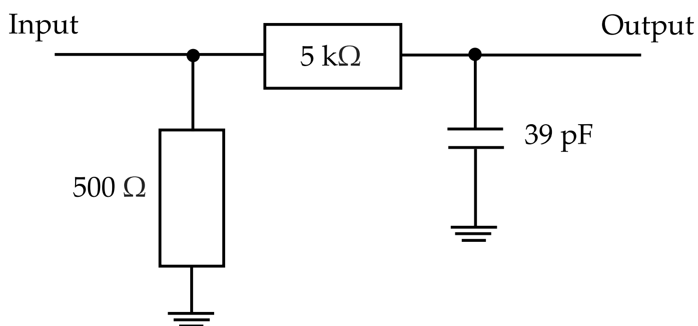

Figure 4.1: The RC filter used to match the output of the phase detector and the input of the PI controller.

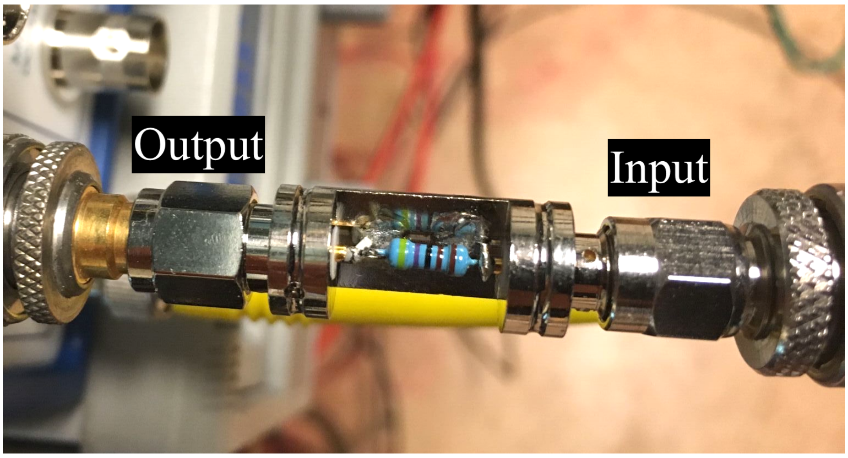

Figure 4.2: A Photograph of one of the RC filters that was built to match the output of the phase detector and the input of the PI controller.

5 Fiber Noise Cancellation System 1

The first fiber that was stabilized during this project is shown in Figure 5.1, and connects the optical table to the vibration isolation platform were the PDH locking cavity is located. The fiber is a 1.0 meter long polarization-maintaining single-mode fiber manufactured by Thorlabs (PM460-HP-FC/APC). Both fiber ends are angled at 8° to prevent unwanted back-reflections. A fiber is used because the vibration isolation platform moves to compensate for vibrations. If the beam instead was sent from the optical table to the vibration isolation platform through the air, these movements would cause a change in the distance between the mirror on the optical table, and the mirror on the vibration isolation platform. This change in distance would frequency modulate the light. Light propagating through the fiber, may however also be affected by the compensating movements of the vibration isolation platform, which induce phase noise that has to be compensated for.

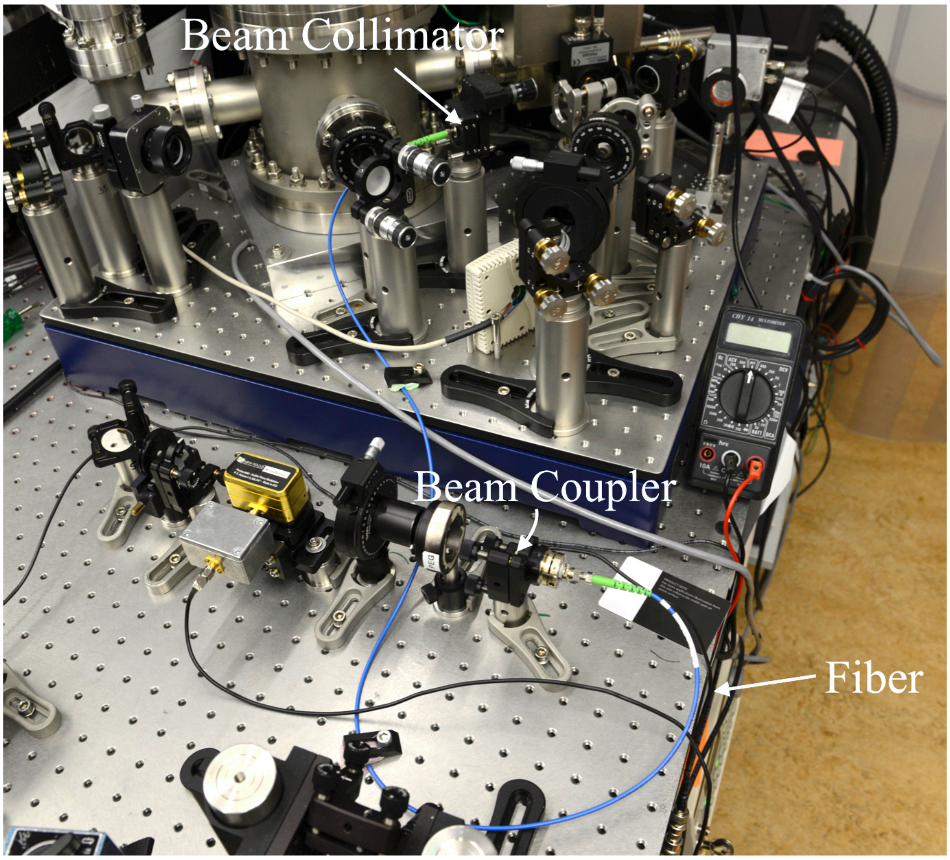

Figure 5.1: The first fiber noise cancellation system was build to cancel phase noise induced by the pictured fiber (blue cable). A beam coupler is used to efficiently couple the beam into the fiber. At the remote end of the fiber, a beam collimator transforms the divergent beam out of the fiber into a collimated beam.

5.1 Equipment

This section specifies the components used for the fiber noise cancellation system. In Table 1, an overview of the components can be seen. Information on some of the key components is then given.

Component	Manufacturer	Model
AOM	Isomet	1205C-2
Beam collimator	Schäfter Kirchhoff	60FC-4-M5-33 [1]
Beam coupler	Schäfter Kirchhoff	60SMS-1-4-M5-33
Beam splitter	Thorlabs	BST10
Directional coupler	Mini-Circuits	ZX30-20-4
D-shaped mirror	Thorlabs	BBD1-E02
Faraday rotator	Leysop	FOI 5/57
High power amplifier	Mini-Circuits	ZHL-32A
Mixer/Phase detector	Mini-Circuits	ZAD-3
Oscilloscope	Teledyne LeCroy	HRO 66Zi
Optical fiber	Thorlabs	PM460-HP-FC/APC
Photodetector	Home-built	-
PI controller	Stanford Research Systems	SIM960
Polarizer	Foctek	GLH8008 [1]
Polarizing beam splitter	Foctek	GPB7008 [1]
Reference Oscillator	Rohde & Schwarz	SML01
Rubidium frequency standard	Stanford Research Systems	FS725
2$\times$Small signal amplifier	Mini-Circuits	ZX60-4016E+
VCO	Rohde & Schwarz	SML01

Table 1: Components fiber noise cancellation system 1.

5.1.1 PI-Controller

A SIM960 analog PID controller from Stanford Research Systems was used. The SIM960 has low noise and is thus good for applications such as laser power and wavelength stabilization, which are noise sensitive. It also has a wide 100 kHz bandwidth [18]. In Figure 5.2 the front panel of the SIM960 can be seen. The filtered output from the phase detector should be connected to the Measure input. The Setpoint input is left open and instead an internal setpoint of 0 V is chosen in the Setpoint menu. The control signal is extracted from the BNC connector in the OUTPUT section, which also has a button that switches between Manual and PID Control. The control voltage to the signal generator (SML01) should be limited to ± 1 V$_p$. This can be done in the Limits menu. A BNC connector at the back of the controller provides the error signal, which is limited to ± 10 V$_p$. The procedure for tuning a controller is given in Section 2.2.2. The derivative term of the controller was not used.

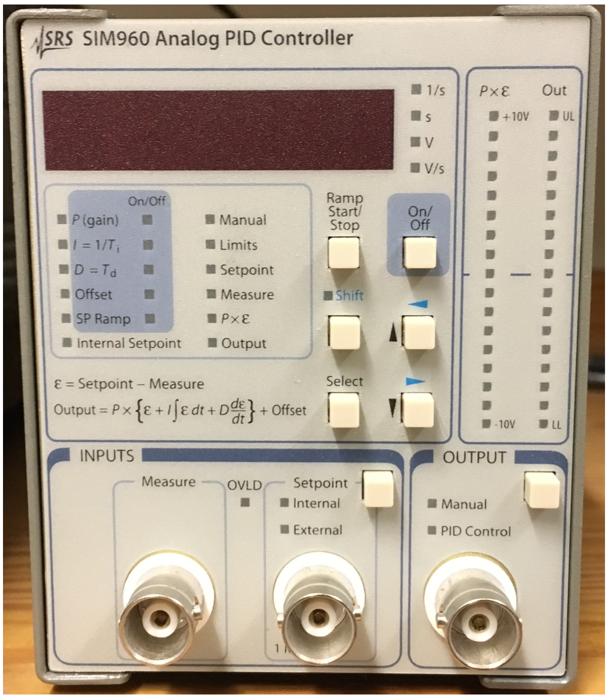

Figure 5.2: The front panel of the SIM960 Analog PID Controller.

5.1.2 Signal Generators

Two SML01 signal generators manufactured by Rohde & Schwarz were used as the VCO and the reference oscillator. The SML01 has a frequency range of 9 kHz-1.1 GHz, and can thus provide the driving frequency to the AOM at 60 MHz, as well as the reference frequency at 120 MHz. It has a sufficiently low SSB phase noise of -128 dBc, and will therefore not significantly add phase noise to the laser. The SML01 also has the ability to be frequency modulated by an external source with a modulation bandwidth of 1 MHz. The fiber noise cancellation systems requires a minimum modulation bandwidth of 20 kHz [9], which the SML01 thus can provide.

5.1.3 Acousto-Optic Modulator

The AOM used for this fiber noise cancellation system was the Isomet 1205C-2. This model has a center frequency of 80 MHz, an RF bandwidth of 30 MHz and an acoustic velocity of 3.63 mm/μs. The modulation bandwidth for a beam diameter of 2 mm, is 1 MHz at MTF (depth of modulation) 0.5. The modulation bandwidth of the AOMs is thus much higher than the phase noise bandwidth, which is necessary for the fiber cancellation system to work properly.

5.1.4 Photodetector

The photo detector used for this fiber noise cancellation system was home-built. It has a bandwidth of 100 MHz. In Figure 5.3, a photograph of the photodetector can be seen.

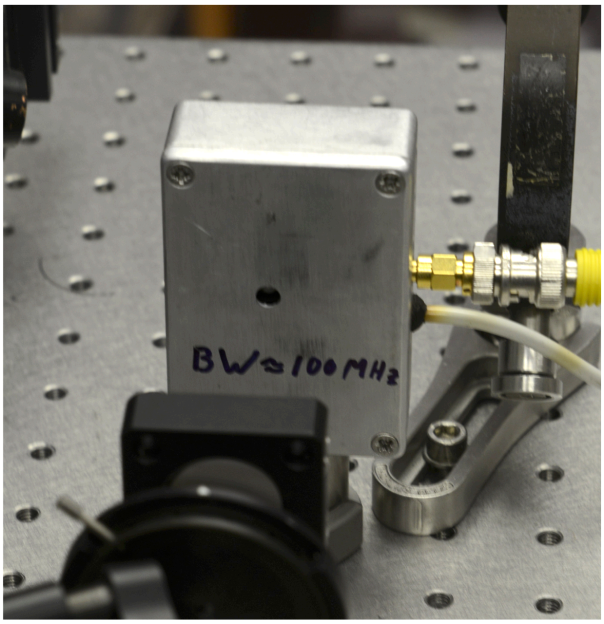

Figure 5.3: The home-built photodetector.

5.2 The Experimental Setup

The setup for the first fiber noise cancellation system is shown in Figure 5.4. It is not possible to evaluate the performance of the system in the same way as Anders Rönnholm did [9]. He measured the frequency spectrum of the beat note between the light directly from the laser, and the light from the remote end of the fiber. This approach would require sending the beam from the vibration isolation platform back to the optical table. The compensating movements of the vibration isolation platform would then frequency modulate the light as already mentioned. Instead I found an alternative approach previously used at the Institute for Quantum Electronics, ETH Zurich [13]. By inserting a directional coupler after the photodetector, the measured beating signal could be sent both to the phase detector, and observed on an oscilloscope. This measurement tells us how noisy the beating signal on the photodetector is, which comes from light that has passed twice through the fiber. It does not tell us if the fiber noise at the remote end of the fiber has been canceled. We do however feel confident that if the two way fiber phase noise is canceled, so is the single pass.

The beam enters the noise cancellation system through a filter wheel, which can be used to adjust the optical power going into the system. A difference from the test setup is the optical isolator, which consists of a polarizing beam splitter (**a**), a Faraday rotator (**b**) and a polarizer (**c**). The isolator only allows light through in the forward direction, preventing unwanted back-reflected radiation from reaching the laser, which could destabilize it. The polarizing beam splitter also picks off the back-reflected +1st and 0th order beams and sends them to the photodetector. The EOM placed before the fiber has nothing to do with the noise cancellation, but it serves to generate the sidebands needed to stabilize the laser with the PDH technique and is thus crucial. For the cancellation system to work properly, the +1st and 0th order beams from the AOM have to propagate a long enough distance to be efficiently separated by the mirror. It is desirable to have an extinction ratio of at least 1:1000 [19], i.e, no more than 0.1% of the power in the 0th order beam should end up in the +1st order beam, and vice versa. The EOM and the optical isolator was therefore positioned to maximize the distance between the

AOM and the mirror that retro-reflects the 0th order beam; a distance of 28.5 cm was achieved. The VCO that drives the AOM was set to have a maximum frequency deviation of ± 15 kHz around a center frequency of 60 MHz, and the reference oscillator frequency was therefore set to 120 MHz. The beating signal on the photodetector will thus be at 120 MHz. The bandwidth of the photodetector is 100 MHz, and the reason for not choosing a lower driving frequency for the AOM, is because the AOM efficiency drops for frequencies below 60 MHz. Both the reference oscillator and the VCO were locked to a 10 MHz rubidium frequency standard with an Allan Variance [20] less than $2 \cdot 10^{-11}$ at one second.

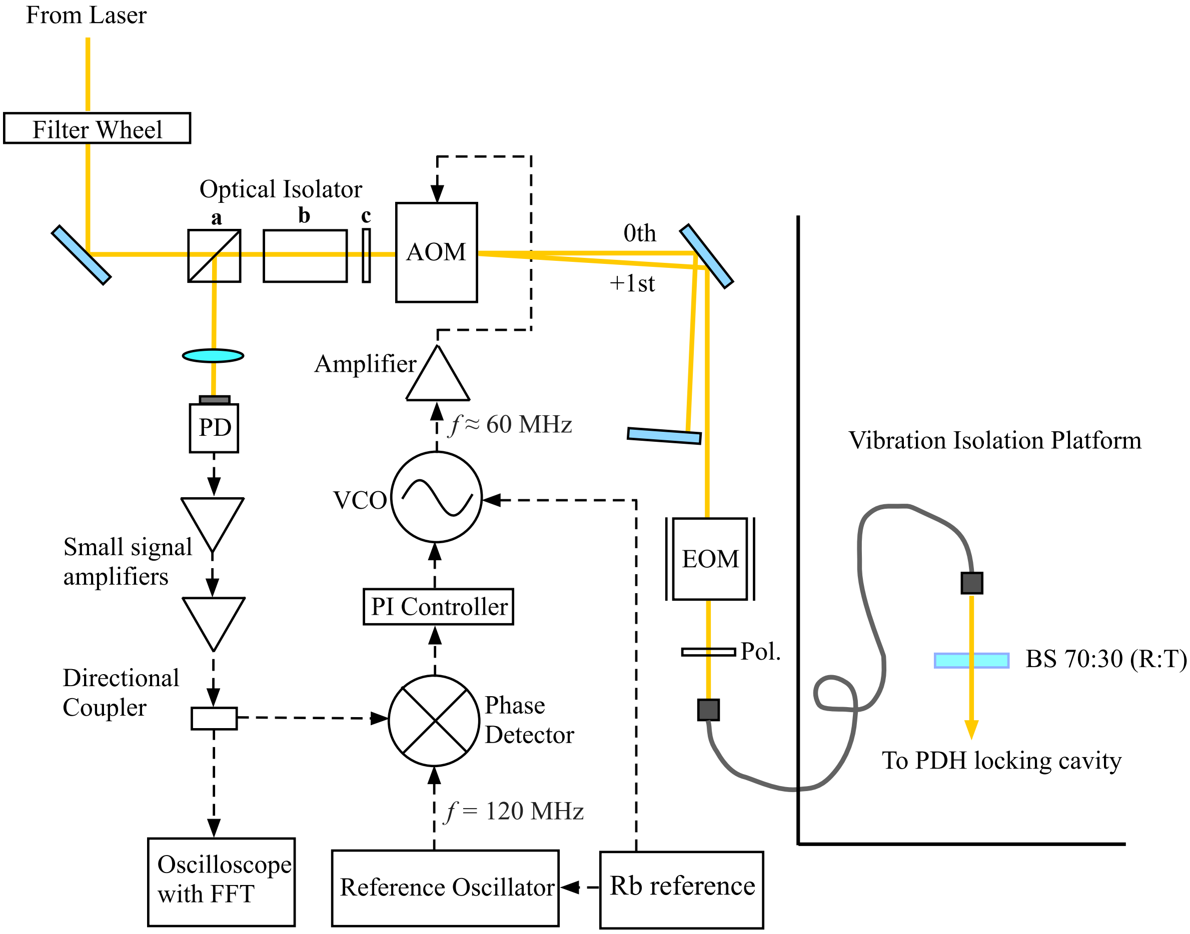

Figure 5.4: Fiber noise cancellation setup for the fiber guiding the light up to the vibration isolation platform.

5.2.1 Bypassing the Double Pass AOM

At first, the beam going into the cancellation system was quite divergent and it was hard to separate the +1st and 0th order beams efficiently. This also made it difficult to couple the +1st order beam into the fiber. The beam quality was degraded by a double pass AOM placed in the beam path before the light enters the cancellation system through the filter wheel. This AOM is not depicted in Figure 5.4, because it is not part of the fiber noise cancellation system, but shown in an overview of the whole laser setup in [1]. The double pass AOM can be used to shift the frequency of the beam to the PDH locking cavity. Previous experiments have used this feature, but not such experiments are planned at the moment, so this AOM was bypassed. It was then easy to get the +1st order beam through the fiber.

5.2.2 Optimizing the Reflected First Order Power

It turned out to be difficult to get a high enough power in the +1st order beam on the photodetector. A beating signal was only observed if the laser power going into the system was increased by a factor of about 20 by turning the filter wheel. But, decreasing the attenuation on the filter wheel would also allow more of the back reflected light to reach the laser, so this is not an optimal solution. The main reason that the +1st order beam was not efficiently reflected back to the photodetector, was the beam splitter after the fiber, and the geometry of the setup, see Figure 5.5a. The beam splitter was measured to have a splitting ratio of roughly 15:85 (Reflection:Transmission). This means that only $2-3\%$ of the output from the fiber can be used for the back coupling, since the light reflects of the beam splitter twice. To optimize the power in the reflected +1st order beam, it was decided to modify the setup as in Figure 5.5b. A back of the envelope calculation showed that it would be optimal to have a 70:30 (Reflection:Transmission) beam splitter after the fiber. If a beam splitter with an even higher reflectivity was chosen, more of the +1st order beam would of course be reflected. But then the desired 40 μW in the beam going to the PDH locking, would not be obtained without decreasing the attenuation on the filter wheel, hence the 70:30 beam splitter was used. Rearranging the setup also meant that time had to be spent realigning the beam to the PDH locking cavity. After the setup had been modified, the power in the 0th and +1st order beams was measured to 40 μW and 20 μW, respectively, which is enough to detect a good beating signal and for the system to work well. For the phase detector to provide a DC voltage proportional to the phase difference between the two input signals, it is important for the RF input power level to be at least +1 dBm. Otherwise the phase detector will not operate in saturated mode, and provide an output voltage proportional to both phase and amplitude of the RF input. The beating signal was therefore amplified so that the signal sent to the phase detector had a power level of +3 dBm. The amplitude of the beating signal did not change much over time, unlike for the test system where this was a problem.

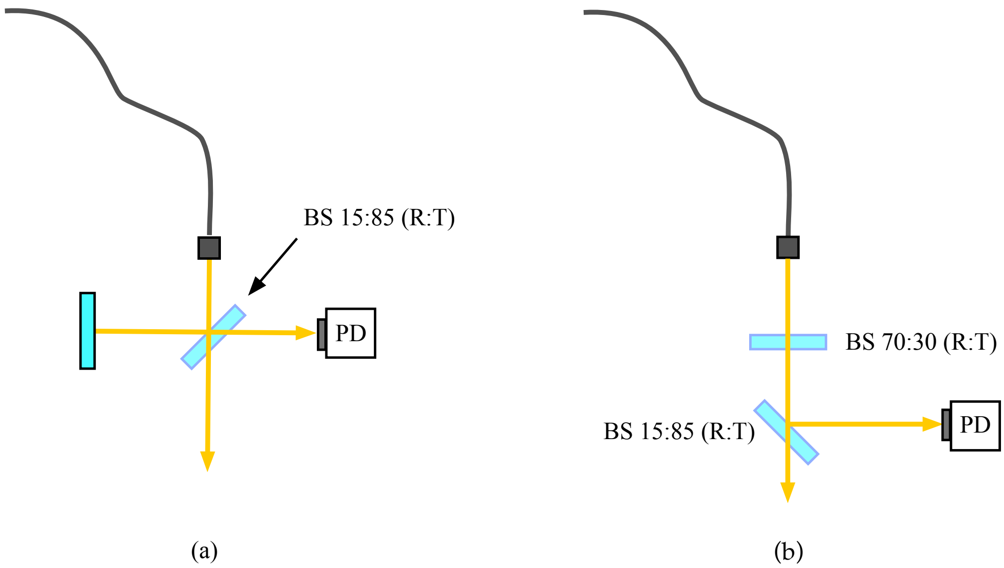

Figure 5.5: The setup after the fiber on the vibration isolation platform as it has been over the last years (a) and the modified setup (b). The photodetector (PD) is used to measure the power after the fiber.

A photo of a part of the fiber cancellation system is shown in Figure 5.6.

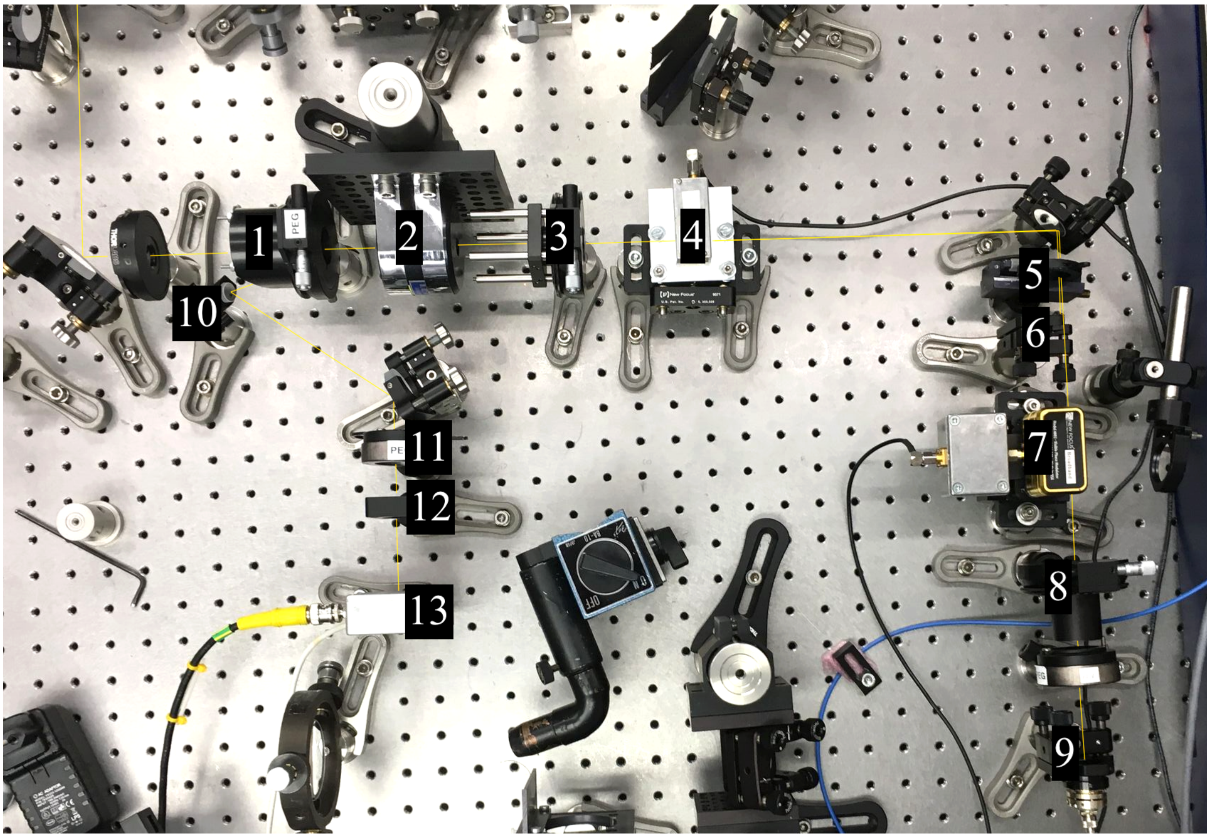

Figure 5.6: The beam enters the fiber noise cancellation system in the top left corner of the photograph. The optical isolator consists of a polarizing beam splitter (1), a Faraday rotator (2) and a polarizer (3). The beam then passes the AOM (4). The pinhole (5) is used to block all other orders except the +1st and 0th. The D-shaped mirror (6) retro-reflects the 0th order. An EOM (7) is used to modulate the laser beam for the PDH locking. A polarizer (8) makes sure that the polarization entering the optical fiber is purely linearly polarized. The beam coupler (9) is used for efficient coupling into the fiber. The back-reflected signal is picked off by a 1/2" mirror placed in a 45° mount (10). Diffraction orders other than the +1st and 0th are blocked from reaching the photodetector by the pinhole (11). A lens (12) focuses the light onto the photodetector (13).

5.3 Evaluating the Performance of the Noise Cancellation System

When the noise cancellation system was off, the error voltage from the PI controller varied between ± 200 mV. The maximum and minimum error voltage values correspond to the inputs to the phase detector being $\pm 180°$ out of phase. In Figure 5.7a, the error voltage is shown over a 4 s period. The voltage changes at a slow rate, except for some small faster fluctuations. This implies that there is not much phase noise on the beating signal. When the noise cancellation system was on, the error signal voltage was clearly reduced and kept close to 0 V, see Figure 5.7b.

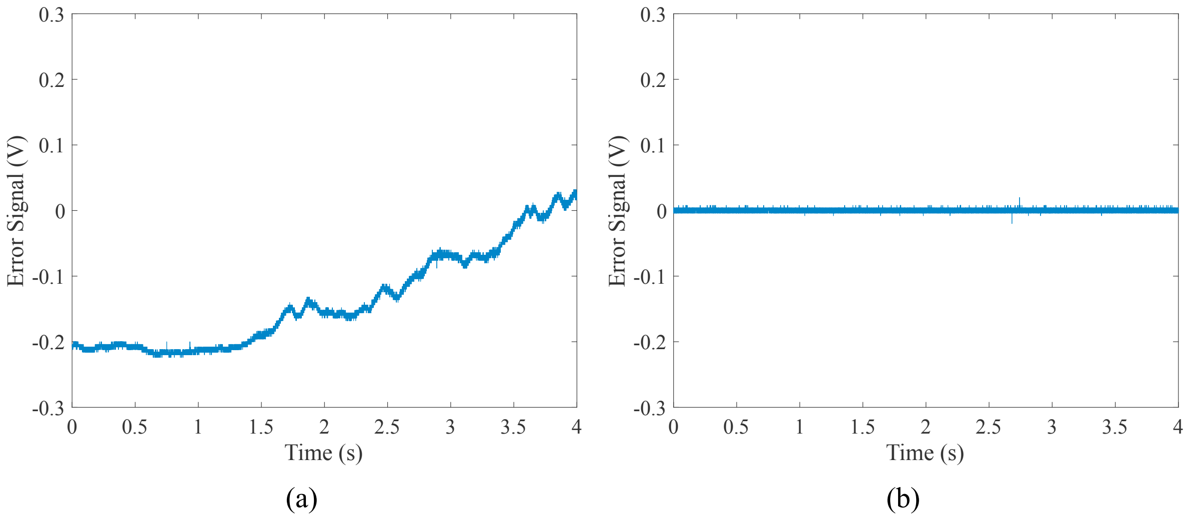

Figure 5.7: A comparison between the error signal from the PI controller (a) without and (b) with the cancellation enabled.

In Figure 5.8, the frequency spectrum of the beating signal with and without noise cancellation is shown. The system seems to be canceling some noise. Two low-power side peaks are suppressed, and the spectrum is smoothened out when the noise cancellation is active. It is however not very evident from this figure how well the noise cancellation is working, since there is very little noise to begin with. It was surprising to us that the spectrum is so narrow even without noise cancellation. Figure 5.9 reveals a linewidth of about 50 Hz at -40 dB from the carrier peak power, and the linewidth is limited by the resolution of the measurement. The group at ETH Zurich that also measured the frequency spectrum of the beating signal using a directional coupler, demonstrated a kHz broadening of the spectrum from fiber noise [13]. But they used a 25 m long fiber. Our fiber is only 1.0 m, and a shorter fiber will induce less noise. Other contributing factors to the narrow frequency spectrum, could be that the laboratory temperature is well regulated and that loud equipment is kept in a machine room next door. Mechanical vibrations because of the compensating movements of the vibration isolation platform do not seem to effect the light propagating through the fiber much.

In all measured spectra, low-power peaks were observed at ± 1.9 kHz and ± 3.8 kHz from the carrier frequency. These peaks were not suppressed at all by the cancellation system and their origin is unknown.

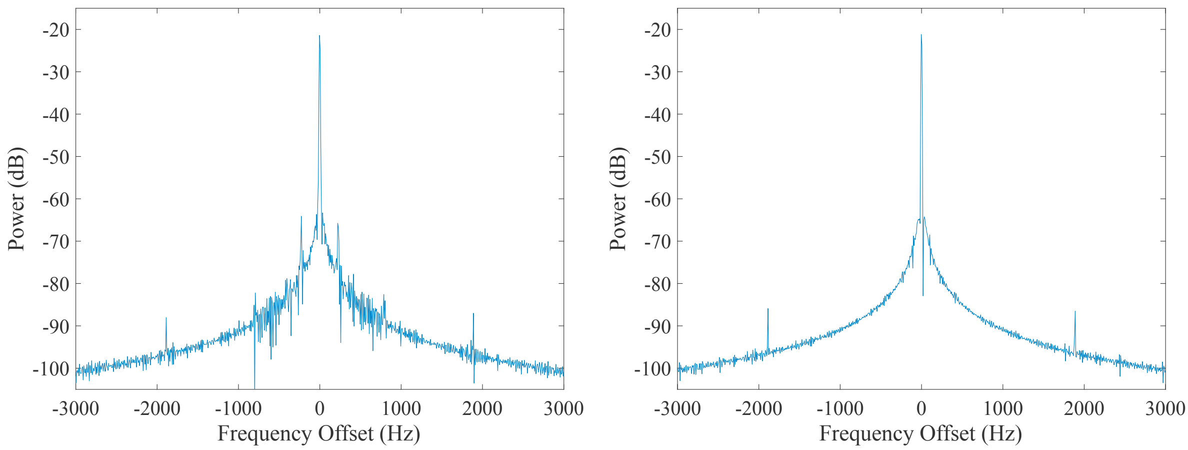

(a) (b)

Figure 5.8: Comparison between the frequency spectrum of the beating signal without (a) and with (b) noise cancellation, for a 6000 Hz span around the carrier. The horizontal axis represents the frequency offset from 120 MHz.

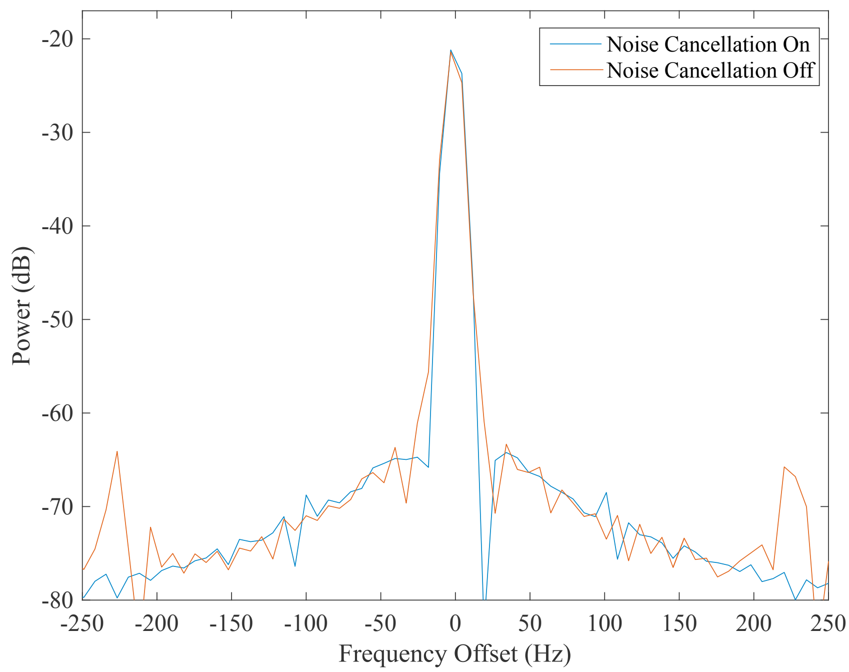

Figure 5.9: Comparison between the frequency spectrum of the beating signal with and without noise cancellation, for a 500 Hz span around the carrier. The horizontal axis represents the frequency offset from 120 MHz.

To better verify that the cancellation system was actually working, a small speaker generating a 1 kHz tone was put next to the fiber. Peaks at ± 1 kHz from the carrier frequency then showed up in the spectrum. With the fiber noise cancellation turned on, these 1 kHz peaks were suppressed almost entirely, see Figure 5.10. It was therefore concluded that a functioning fiber noise cancellation system had been assembled.

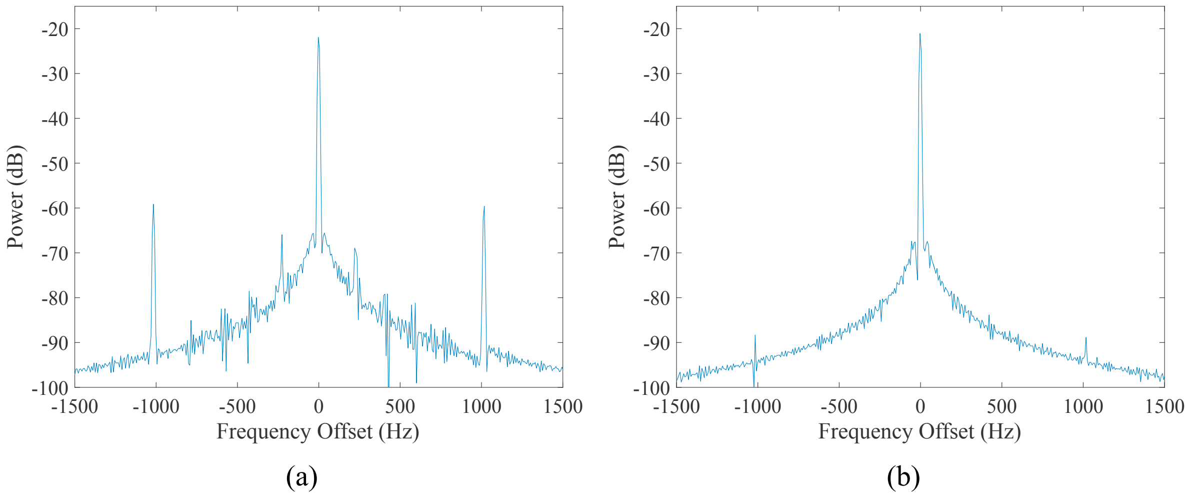

Figure 5.10: Comparison between the frequency spectrum of the beating signal without (a) and with (b) noise cancellation, for a 3000 Hz span around the carrier. Here a small speaker generating a 1 kHz tone has been put next to the fiber. The horizontal axis represents the frequency offset from 120 MHz.

6 Fiber Noise Cancellation System 2

The second fiber that was stabilized during this project is shown in Figure 6.1, and connects the laser table to the cryostat table. The fiber is a 25 meter long polarization-maintaining single-mode fiber manufactured by Schäfter-Kirchhoff (PMC-630-3.8-NA012-3-APC-2500-P). Both fiber ends are angled at 8° to prevent unwanted back-reflections.

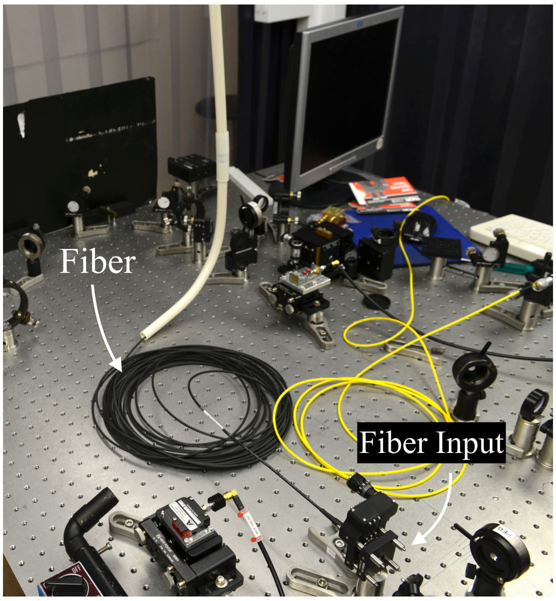

(a) At the laser table, the fiber is guided up through a pipe.

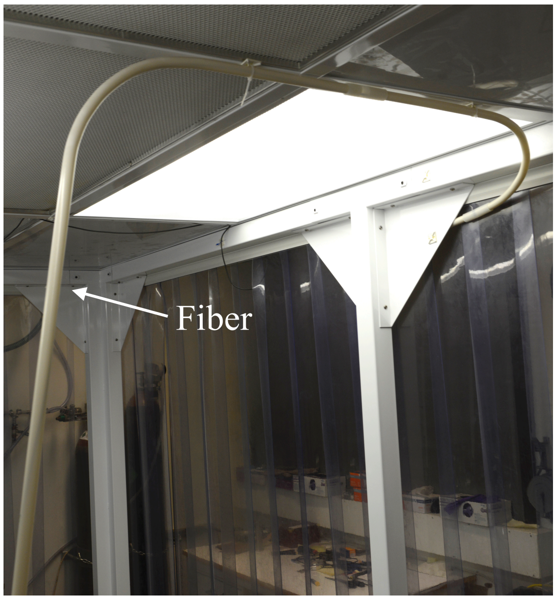

(b) The pipe continues up to the ceiling and towards the cryostat table.

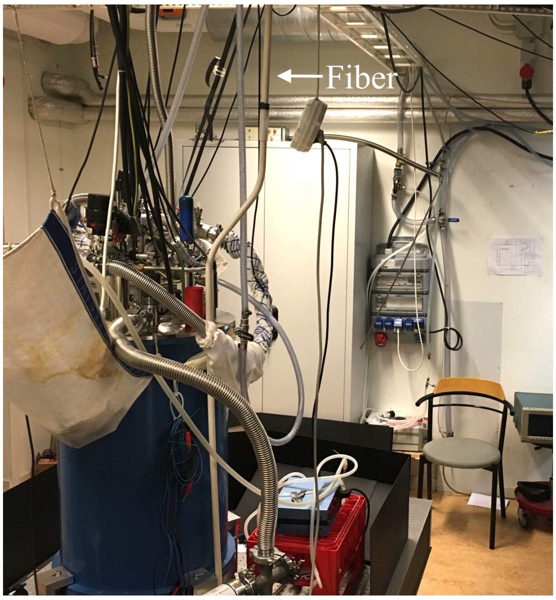

(c) The pipe guides the fiber down to the cryostat table.

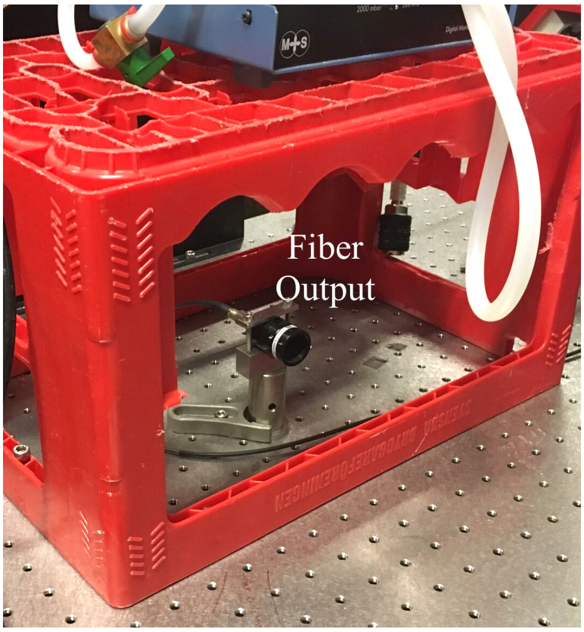

(d) A beam collimator at the remote end of the fiber provides a collimated beam.

Figure 6.1: The second fiber noise cancellation system was build to cancel phase noise induced by the pictured fiber.

6.1 Equipment

This section specifies the components used for the fiber noise cancellation system. In Table 2, an overview of the components can be seen. Information on some of the key components is then given.

Component	Manufacturer	Model
AOM	Isomet	1205C-2
Beam sampler	Thorlabs	BSF10-A
Beam splitter	Thorlabs	BSN10
Directional coupler	Mini-Circuits	ZX30-20-4
High power amplifier	Mini-Circuits	ZHL-3A
Optical fiber	Schäfter-Kirchhoff	PMC-630-3.8-NA012-3-APC-2500-P
Oscilloscope	Teledyne LeCroy	HRO 66Zi
Phase detector	Mini Circuits	ZRPD-1
Photodetector	Thorlabs	Custom build (B2200)
PI-controller	New Focus	LB1005
Reference oscillator	Rohde & Schwarz	SMIQ03B
Rubidium frequency standard	Stanford Research Systems	FS725
Small signal amplifier	Mini-circuits	ZX60-33LN+
VCO	Rohde & Schwarz	SML01

Table 2: Components fiber noise cancellation system 2.

6.1.1 PI-Controller

For this fiber noise cancellation system, an LB1005 High-Speed Servo Controller from New Focus was used. This is a controller that is well suited for frequency and intensity stabilization of laser systems and has a large 10 MHz bandwidth [21]. The front panel of the LB1005 can be seen in Figure 6.2. The filtered output from the phase detector should be connected to the A input. The -B input is auto-terminated when left open. The output voltage limits of the controller can be adjusted with trimpots located on the rear panel. The control voltage to the signal generator (SML01), should be limited to ± 1 V_p. Because the output of the LB1005 has an impedance of 50 Ω and the modulation input on the SML01 is high impedance, the output voltage limits of the controller should be set to ± 0.5 V_p. The error voltage can be monitored from the Error Monitor output, which has a voltage range of ± 10 V. An important feature of the LB1005 is the Int Hold input. By applying a voltage > 2.4 V to this input, the error signal input to the PI-filter can be turned off, while holding the integrator output voltage at its current value. This is necessary for this fiber noise cancellation system, which has to be turned on and off for the slow light cavity experiments.

Figure 6.2: The front panel of the LB1005 High-Speed Servo Controller.

6.1.2 Signal Generators 5.1.2

An SML01 signal generator was used as the VCO. The SML01 has already been described in Section 5.1.2. An SMIQ03B manufactured by Rohde & Schwarz was used as the reference oscillator. The SMIQ03B has a frequency range of 300 kHz-3.3 GHz, an SSB phase noise of -116 dBc and a modulation bandwidth of 2 MHz. It should therefore be a suitable choice for the cancellation system.

6.1.3 Photodetector

For the second fiber noise cancellation system, a custom-made PDA10BS-AC photodetector (B2200) was used. The detector was manufactured by Thorlabs and is similar to the PDB110A-AC model. The transimpedance is $1.65 \cdot 10^4$ V/A at 50 Ω, and the AC saturation power is 200 μW.

6.1.4 Acousto-Optic Modulator

An Isomet 1205C-2 was used for this fiber noise cancellation system as well. See Section 5.1.3 for more information on this AOM.

6.1.5 Phase Detector

The two phase detector that were available were a ZRPD-1+ and an RPD-2, both from mini circuits. Both appeared to be working correctly and giving the same output when applying two 120 MHz signals to the inputs. Because there were suspicions that the RPD-2 had behaved abnormally in the past, I chose the ZRPD-1+. I did however later realize that this phase detector was only specified for the frequency range 1-100 MHz, and may therefore not have been the best choice, since we want to compare two 120 MHz signals. It may have been better to use the RPD-2, which is specified for frequencies up to 150 MHz.

6.2 The Experimental Setup

The experimental setup for the second fiber noise cancellation system is shown in Figure 6.3. This setup closely resembles the setup for the first fiber noise cancellation system. Once again the performance of the system was evaluated by measuring the frequency spectrum of the beating signal on the photodetector using a directional coupler and an oscilloscope. The VCO that drives the AOM was setup to have a maximum frequency deviation of ± 15 kHz around a center frequency of 60 MHz and the reference oscillator was set to 120 MHz. Both the VCO driving the AOM and the reference oscillator were locked to a rubidium frequency standard with an Allan Variance less than $2 \cdot 10^{-11}$ at one second. The mirror (M1) was positioned so that it would rather let some of the 0th order beam pass than reflect some of the +1st order beam. An aperture (A1) was then used block the small fraction of the 0th order beam that passed M1. An aperture (A2) after the AOM blocks all orders except the 0th and +1st order. During the measurements on this system, the power in both the +1st and 0th order beams on the photodetector was about 20 μW. The beating signal was amplified to +1 dBm before being fed to the phase detector.

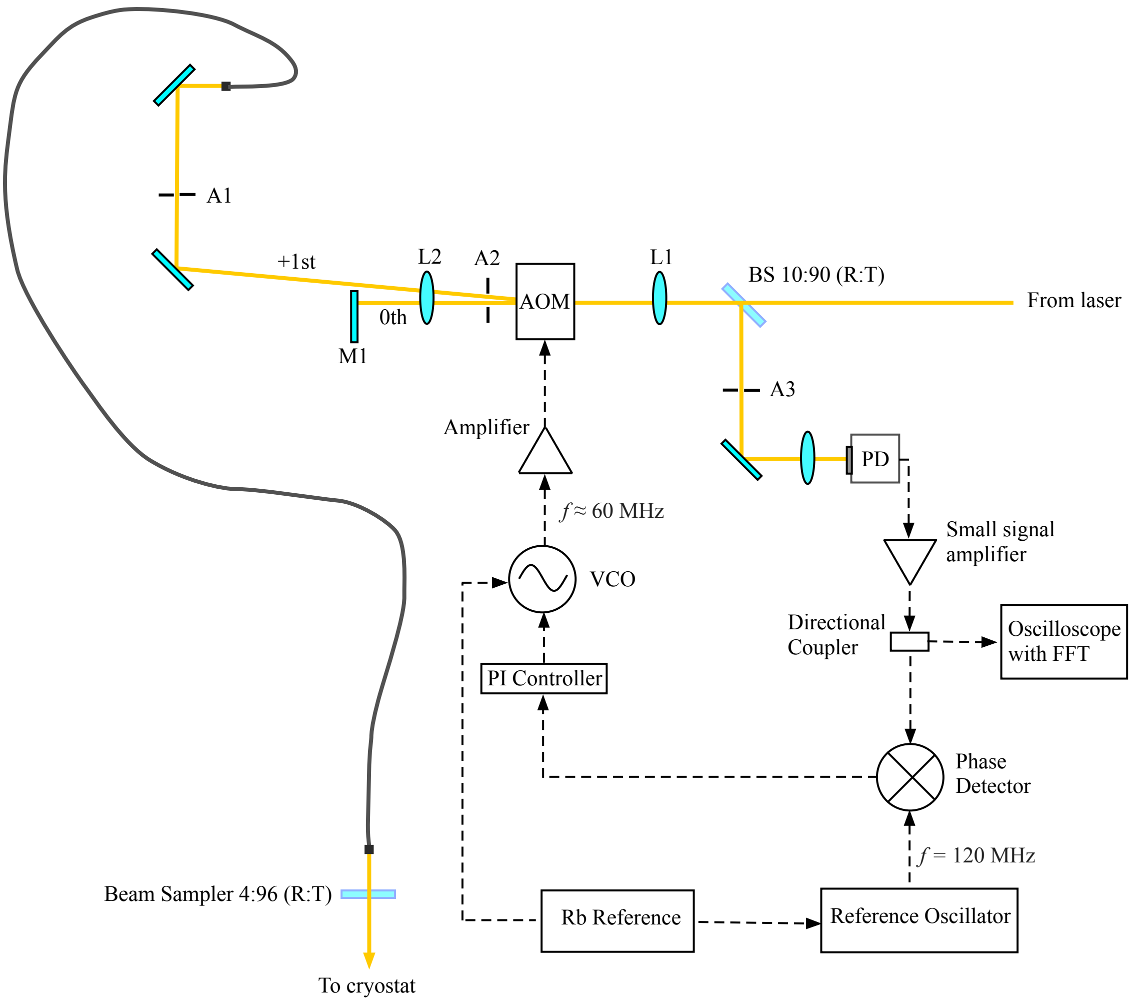

Figure 6.3: Fiber noise cancellation setup for the fiber connecting the laser table and the cryostat table.

Note that when measuring the performance of this system, the mirror (M1) that retro-reflects the 0th order beam was placed before the lens (L2), and not directly after as shown in Figure 6.3. The beam is focused by the lens before the AOM (L1), and the lens after the AOM (L2) collimates the beam again. By placing the mirror before L2, the reflected 0th order beam will be divergent, and then clipped by the AOM, as the beam diameter is larger than the AOM aperture. This results in a very large unnecessary loss of power in the 0th order beam on the photodetector.

By beating the +1st order beam with a higher power 0th order beam, the measured beating signal should be less sensitive to photodetector noise. This was realized after the performance of the system had been measured, and the retro-reflecting mirror (M1) will therefore be moved to the the position showed in Figure 6.3 for future use of the noise cancellation system. Similarly, the beam splitter (BS) was placed after the lens (L1) during the measurements on this system, and not before the lens as shown in Figure 6.3. This does however not affect the power on the detector as much, since the beams are focused shortly after reflecting of the beam splitter.

6.2.1 Changing the AOM

The AOM that has been used before the fiber over the last years, is an AA OPTO-ELECTRONIC AA.ST.360/B200/A0.5-vis operating at 360 MHz. The beating signal that contains information on the phase error would then be at 720 MHz, since the AOM is passed twice. This frequency is higher than any of our photodetectors can detect, and in general the noise in photodetectors with high enough bandwidth is much larger. Therefore, the AOM had to be replaced. An Isomet 1205C-2 operating at 60 MHz was therefore inserted, giving a beating signal at 120 MHz. The AOMs have similar acoustic velocities and the existing computer code used for tailoring specific laser pulses should then work with the new AOM as well.

6.2.2 Choosing the Beam Splitters

The beam splitters for this setup were chosen to maximize the optical power reaching the cryostat, since a high power is desirable for efficient spectral hole burning. A 10:90 (R:T) beam splitter was inserted before the AOM and a 4:96 (R:T) beam sampler was inserted after the fiber. The power should then only drop by a factor of 0.86 because of the cancellation system. It was however later realized that the splitting ratio of the beam splitter labeled as a 10:90 (R:T) beam splitter, was actually closer to 20:80 (R:T). This beam splitter will therefore most likely be replaced in the future.

If one wants to build a fiber noise cancellation system that cancels fiber noise as efficient as possible, this choice of beam splitters is not optimal. In that case, the beam sampler would be replaced with a beam splitter which reflects more light from the remote end of the fiber.

An alternative setup used by [13, 22] that does not need a beam splitter before the AOM was found when writing this thesis. The only loss of optical power because of the cancellation system would then be from the beam sampler at the remote end of the fiber. This would increase the power reaching the cryostat compared with the setup I have assembled.

6.2.3 Electronically Turning the Stabilization On/Off

For this fiber noise cancellation system, a method to electronically turn the cancellation system on and off had to be investigated. When performing laser locking experiments to a slow light cavity, a spectral hole in the absorption profile of the ions in the crystal is first burnt. During the burning process, a sequence of laser pulses is sent. The fiber noise cancellation system is not able to cope with pulsed radiation, and should preferably be turned off. After the hole burning process is completed, the fiber noise cancellation system should be turned on, to provide a more frequency stable signal for the slow light cavity locking. The LB1005 PI controller has an Int Hold input (described in Section 6.1.1) that can be used for this. When applying a voltage to this input, the PI controller indicated that the system was not locked, and when removing the voltage the PI controller indicated that the system was locked again. It was therefore concluded that the Int Hold input could be used for turning the noise cancellation system on and off.

6.2.4 Minimizing the Unwanted Reflection

Unwanted reflections from the AOM and the lens (L2) that reached the photodetector was a problem. Initially the power in the unwanted reflections was roughly 1/8 of the power in the +1st order beam on the photodetector. By slightly angle both the AOM and the lens, and using an aperture (A3) to block the unwanted reflections, this ratio could be lowered to around 1/25 instead. When the aperture was carefully placed, so that the +1st order beam could pass, while as much as possible of the unwanted reflections was blocked, a clean 120 MHz beating signal was observed. If the pinhole was opened slightly, allowing more of the unwanted reflection to reach the photodetector, the beating signal was not a clean 120 MHz sine anymore.

6.3 Evaluating the Performance of the Noise Cancellation System

Figure 6.4a shows the error voltage from the PI controller over a 0.1 s period without noise cancellation. The error voltage varies much faster compared with the error voltage for fiber noise cancellation system 1. This implies a beating signal with more phase noise, which is expected. A longer fiber will induce more phase noise. The longer fiber is also more exposed to mechanical vibrations as it is led up along the ceiling through the pipe, unlike the 1.0 m fiber, which is clamped down to the stable optical tables, compare Figure 5.1 and Figure 6.1. When the noise cancellation system was on, the error voltage from the PI controller was clearly reduced and kept close to 0 V, see Figure 6.4b.

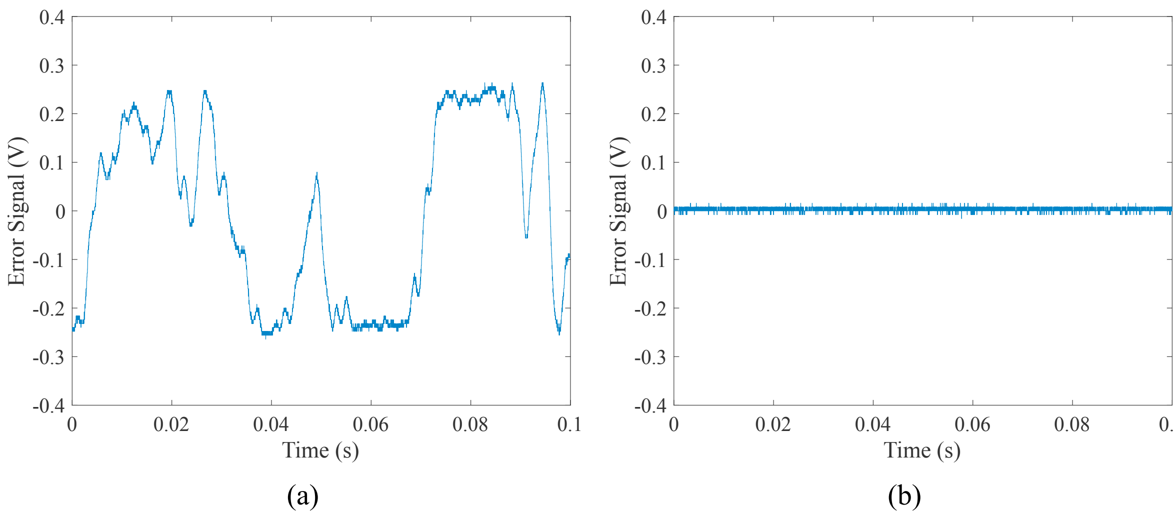

Figure 6.4: A comparison between the error signal from the PI controller (a) without and (b) with the noise cancellation enabled.

Figure 6.5 shows the frequency spectrum of the beating signal with and without noise cancellation for a 6000 Hz span around the carrier. Without noise cancellation, the spectrum is clearly broadened by fiber phase noise. With noise cancellation enabled, most of the signal power is regained in a sharp spectral feature. Figure 6.6, shows that this spectral feature is about 40 Hz wide, and remains narrow to a power level of almost -40 dB from the carrier peak power. The width is limited by the resolution of the measurement. This result is similar to results obtained at ETH Zurich where a similar setup was used [13]. It is however not as good as the results obtained by Long-Sheng Ma et al. [7], whose work the fiber noise cancellation systems described in this thesis is based on. They regained a sharp spectral feature down to almost -50 dB from the carrier peak power.

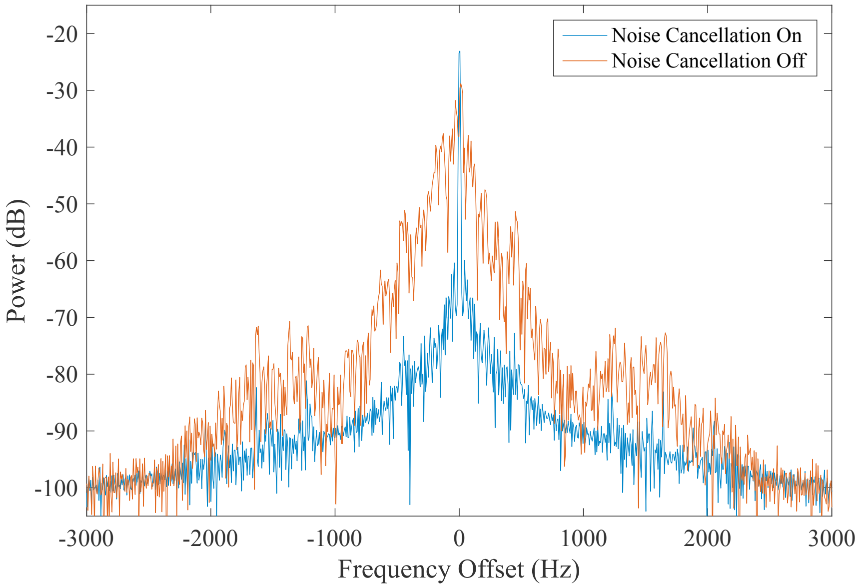

Figure 6.5: A comparison between the frequency spectrum of the beating signal with and without noise cancellation for a 6000 Hz span around the carrier. The horizontal axis shows frequency offset from the carrier frequency at 120 MHz.

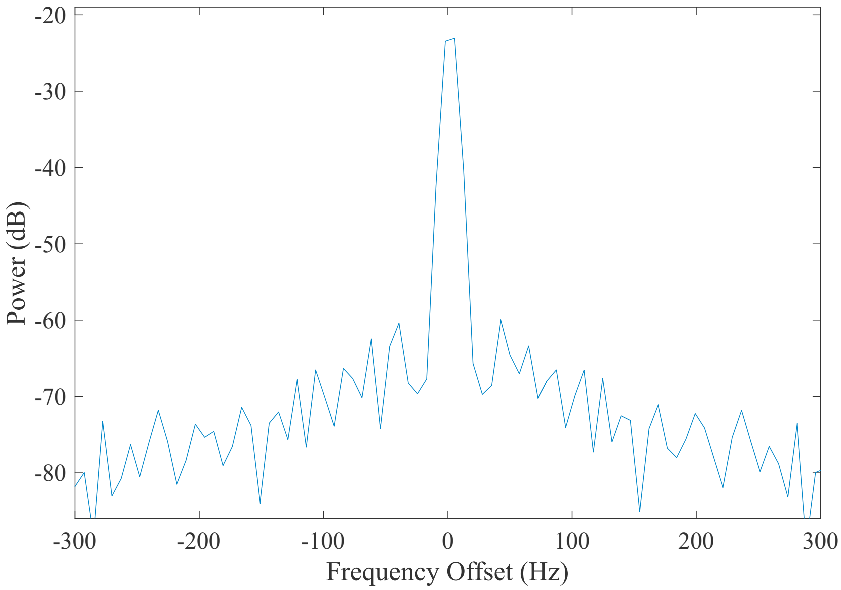

Figure 6.6: The frequency spectrum of the beating signal with noise cancellation. The horizontal axis shows frequency offset from the carrier frequency at 120 MHz.

In Figure 6.7, fiber noise cancellation system 2 is compared to fiber noise cancellation system 1. The beating signal for fiber noise cancellation system 2 is somewhat more noisy. This indicates that it should be possible to improve the performance of fiber noise cancellation system 2 slightly.

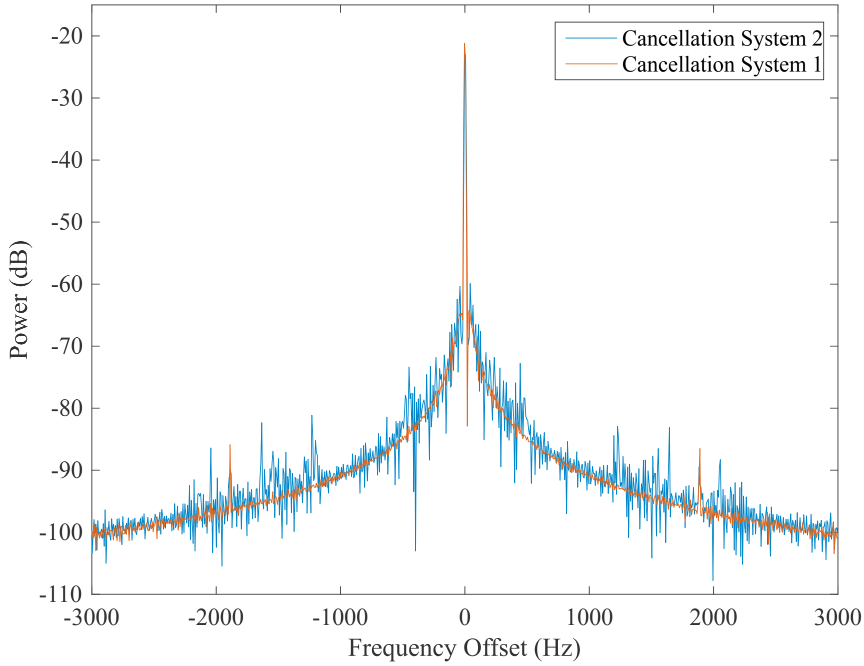

Figure 6.7: Comparison between the frequency spectrum of the beating signal for fiber noise cancellation system 1 and fiber noise cancellation system 2. Both spectra are with noise cancellation enabled. The horizontal axis shows frequency offset from the carrier frequency at 120 MHz.

7 Slow Light Crystal Cavity Laser Locking

The goal of the slow light crystal cavity laser locking experiments was to assemble an experimental setup and attempt to lock the laser to the crystal cavity. An experimental setup was assembled, but unfortunately our AWG that had been behaving strangely for a month, stopped working. Because we suspected that the AWG was at the end of its lifetime, a new AWG of the same model had been bought. We did however not get the new AWG to work properly before the time in the laboratory was up, and the last days were spent troubleshooting instead of attempting to lock the laser to the crystal cavity.

7.1 Equipment

This section specifies the equipment used for the laser locking setup. It only specifies equipment that needs to be added in addition to the standard setup in the laboratory to perform laser locking experiments. The equipment for the fiber noise cancellation system has already been discussed in Section 6.1

7.1.1 Crystal Cavity

The crystal cavity was a 6 mm long yttrium silicate crystal doped with praseodymium at a relative concentration of 0.05%. Both ends of the crystal are equipped with a 95% reflective coating. The crystal is placed in a cryostat, where it is cooled to a temperature of 4 K to increase the lifetime of the hyperfine levels and to remove thermal broadening [4].

7.1.2 Components Overview

Table 3 shows the components that were added for the laser locking experiments.

Component	**Manufacturer**	**Model**
AWG2	Aim-TTi	TGA1244
Beam splitter (BS 50:50 (R:T))	Thorlabs	BSW10
EOM	Linos	PM-25
High Voltage Amplifier	Newport	New Focus 3211
$4\times$Lenses (f = 250 mm)	-	-
Inverter	-	-
$\lambda/2$-plate	-	-
Low-Pass filter	Stanford Research Systems	SR560
Mixer	Mini-Circuits	ZAD-3
Motorized flipper	-	-
Neutral-density filter	Thorlabs	NE40A-A
Photodetector (PD1)	Thorlabs	PDB150A
PI-controller 2	New Focus	LB1005
Polarizer (pol.)	Thorlabs	LPVISB100-MP2
RF switch	Mini-Circuits	ZASWA-2-50DR
Si PIN photodiode	Hamamatsu Photonics	S5973
Variable Gain High Speed Current Amplifier	FEMTO	DHPCA-100
Zoom-beam expander	-	-

Table 3: Components for the laser locking setup.

The ZAD-3 mixer used for the locking setup is the same mixer that was used in the setup for stabilizing the fiber to the vibration isolation platform. I only planned to run the noise cancellation system for the fiber connecting the laser table to the cryostat table during these experiments. A variable gain high speed current amplifier (DHPCA-100) with an Si PIN photodiode (S5973) was used as one of the photodetectors (PD2).

7.2 Experimental Setup

The experimental setup is an extension of the setup used by Teodor Strömberg in his work [4]. Here the fiber noise cancellation system has been integrated and a couple of other components have been added, see Figure 7.1.

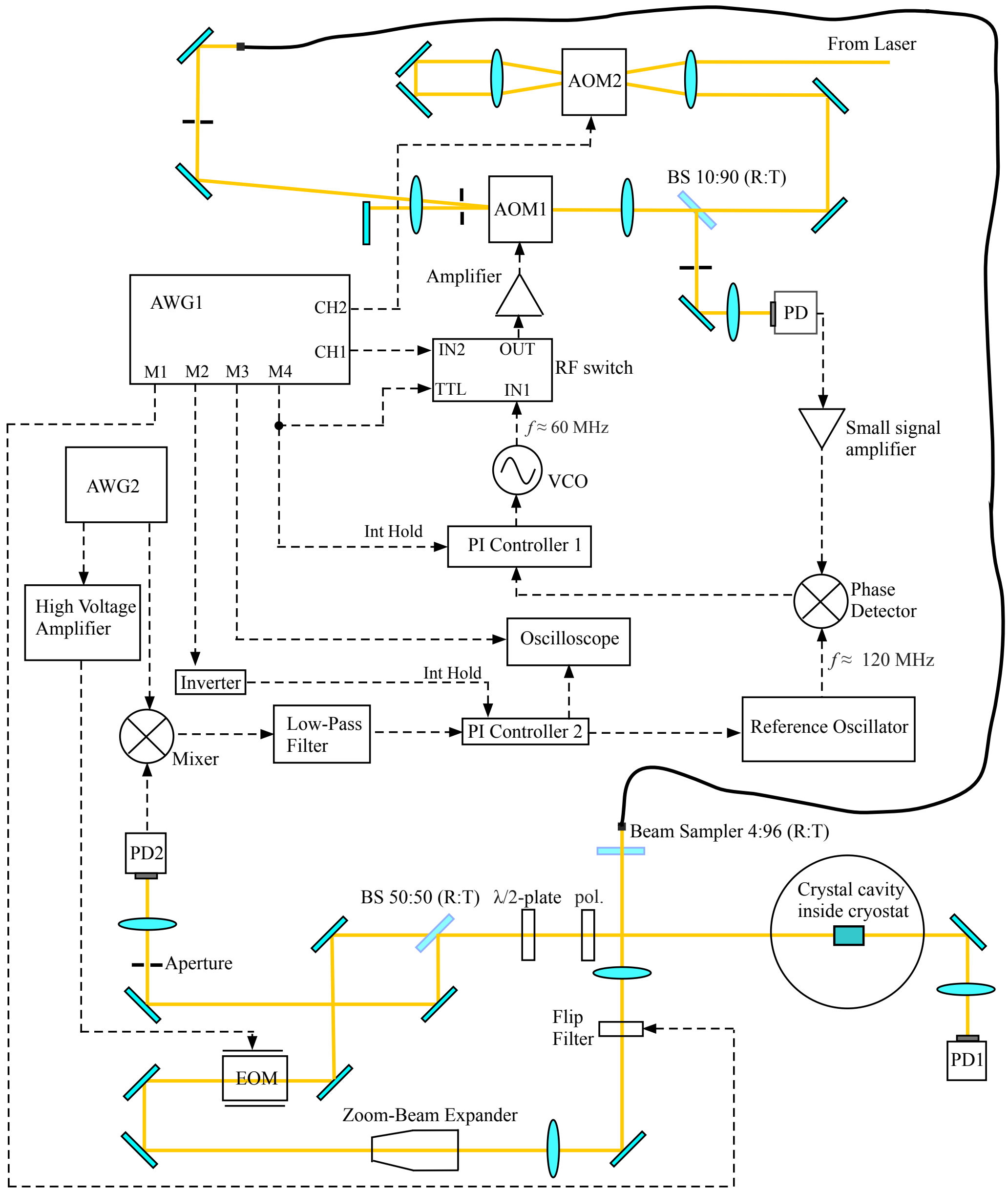

Figure 7.1: Experimental setup for slow light crystal cavity laser locking. The RF switch has two inputs denoted IN1 and IN2, one output denoted OUT, and a transistor–transistor logic (TTL) input which switches between the two inputs. The AWG1 has two waveform outputs, denoted CH1 and CH2, and four marker outputs denoted M1, M2, M3 and M4.

During the spectral hole burning process, a high laser power is necessary. When locking the laser to the crystal cavity, a low power of around 300 nW is believed to be suitable [4]. The fiber noise cancellation system is however not able to run at such low powers, since not enough light will be retro-reflected by the beam sampler. A neutral-density (ND) filter was therefore mounted on a motorized flipper, so that it can be flipped into the beam path after the hole burning pulses, see Figure 7.2. Both a low power to the laser locking and enough power for the fiber noise cancellation can thereby be obtained. The motorized flipper was however unable to flip the filter a far enough to be completely in and out of the beam, because of the rather large beam radius out of the fiber. This problem was solved using a lens that focuses the beam so that it can pass the flip filter without being clipped. A second lens after the flip filter collimates the beam again.

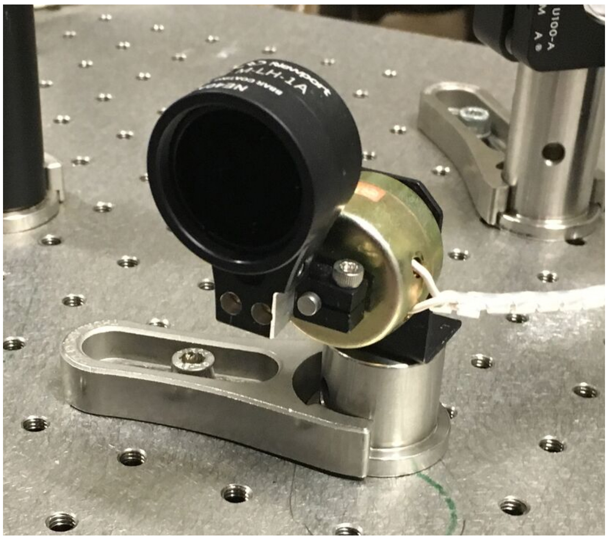

Figure 7.2: Photograph of the motorized flipper with the mounted ND filter.

The zoom beam expander is used backwards to decrease the diameter of the beam. It can also be used to adjust the position and size of the beam waist at the crystal. This is necessary to match the spatial mode of the laser beam to the spatial eigenmode of the crystal cavity. The crystal mirrors are flat, and the wavefronts should then also be flat for the light to be efficiently coupled into the crystal cavity.

The EOM generates the sidebands for the PDH technique and is driven by AWG2, which also sends a phase locked signal with the same frequency to the mixer. These signals can be set with an arbitrary phase offset to compensate for unequal delays in the two signal paths. Before the beam enters the cryostat it passes through a polarizer and a half-wave plate. The polarization of the beam can thus be set along the crystal axis of maximum absorption to get maximum dispersion. The transmitted light can be monitored by the photodetector after the cryostat (PD1). The light that is reflected from the crystal is picked off by the beam splitter and sent to the second photodetector (PD2), that is connected to the mixer. The signal out of the mixer is low pass filtered before being sent to PI controller 2, which FM modulates the reference oscillator of the fiber noise cancellation system. This to hold the voltage out of the low pass filter at zero, thus attempting to lock the laser to a resonance of the crystal cavity.

Each locking attempt was planned to follow the following structure. First, the fiber noise cancellation system is on and PI controller 2 is paused. A marker (M4) is then set high by AWG1 to pause PI controller 1, and also to set the RF switch such that AWG1 controls both AOM1 and AOM2 for the spectral hole burning. When the hole burning is completed, the marker (M4) goes low to unpause PI controller 1 and to set the RF-switch to allow the VCO to take over control of AOM1, so that the fiber noise cancellation system can run. Markers are also set high by AWG1 to the motorized flip filter (M1), which flips into the beam path, to PI controller 2 to unpause it (M2), and to the oscilloscope (M3) so that it starts monitoring the error voltage from PI controller 2. The marker to PI controller 2 is sent through an inverter, meaning that when M2 is set high the voltage at the Int Hold input is set low, and the controller is unpaused.

In Figure 7.3, a photo of the setup on the cryostat table is shown.

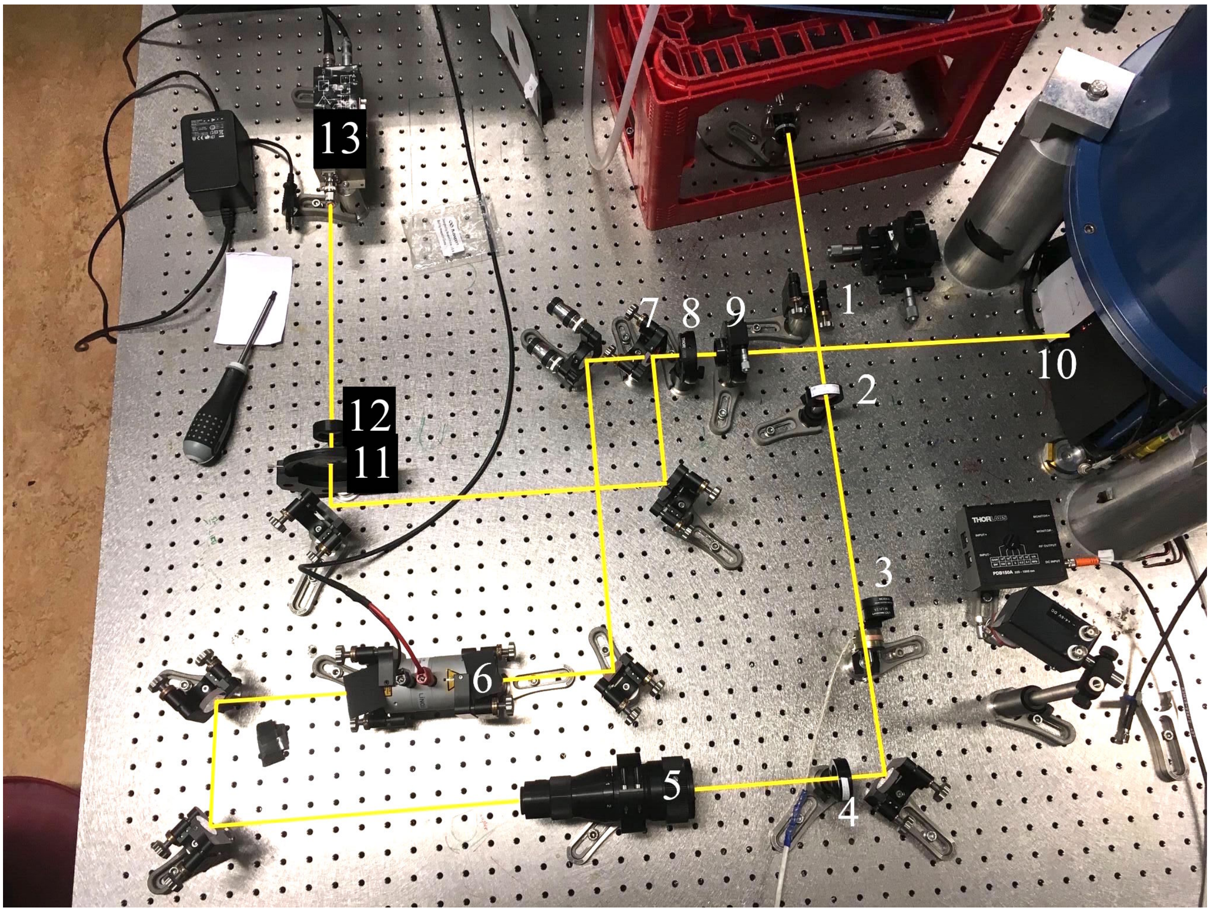

Figure 7.3: A photograph of the cryostat table setup. The beam first passes a beam sampler that reflects 4% for the fiber noise cancellation system (1). It is then focused by a lens (2). The motorized flip filter is (3), which is followed by a collimating lens (4). The beam then passes the zoom-beam expander (5), before passing through the EOM (6). The beam splitter, the half wave plate and the polarizer is (7), (8) and (9) in that order. The beam enters the cryostat through a window (10). The reflected light is picked off by the beam splitter. A pinhole blocks unwanted reflections (11) and a lens (12) focuses the beam onto the photodetector (13).

8 Summary & Outlook

Two fiber noise cancellation systems have been constructed, both showing that the described method can be used to accurately cancel fiber phase noise. It was found that an optical signal propagating through the 1.0 m fiber in our setup was not affected much by fiber phase noise. The fiber noise cancellation system will be running in the laboratory anyways to compensate for the noise that was present, even though it was much less than expected.

For our 25 m fiber, the effects of fiber phase noise were clearly seen in the measured frequency spectrum. The noise cancellation system was able to regain most of the signal in a sharp spectral feature. The mirror that reflects the 0th order beam back to the photo detector, was not optimally positioned during the measurements on this cancellation system, as described in Section 6.2. By moving this mirror, the performance of the noise cancellation system should improve, the question now is by how much. With the current setup in the laboratory, it is possible to use the fiber noise cancellation system for laser locking experiments. For future quantum computation experiments with europium, where pulsed light is used, the setup has to be modified, since the fiber noise cancellation system cannot cope with pulsed light. By moving the pulse shaping AOMs to the table with the cryostat, i.e., after the fiber, it will be possible to run the fiber noise cancellation system while still delivering pulsed radiation to the experiment [19].

When writing this thesis I came across a slightly different fiber noise cancellation setup used by [13, 22]. This setup would be beneficial for stabilizing the 25 meter fiber, and is shown in Figure 8.1. Here, the 0th order of the reflected +1st order beam, and the -1st order of the reflected 0th order beam is overlapped on the photodetector instead.

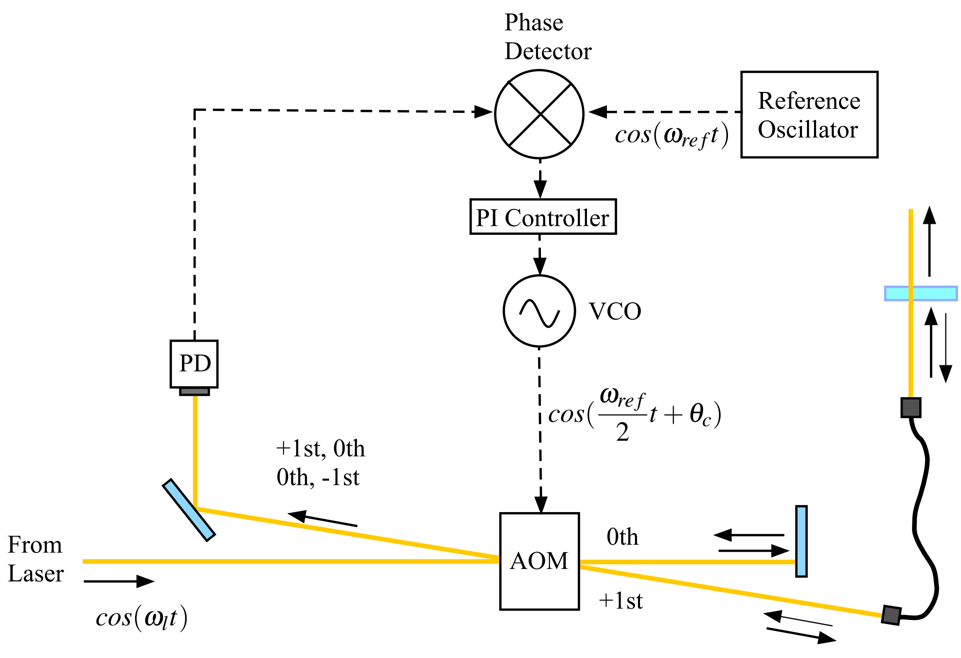

Figure 8.1: Alternative fiber noise cancellation setup.

The overlapped beams on the photodetector could then with the same reasoning and designations as in Section 2.2.5 instead be described by

$$E_1 = cos\Big[(\omega_l + \frac{\omega_{ref}}{2})t + \theta_c + 2\theta_f\Big]$$
$$E_2 = cos\Big[(\omega_l - \frac{\omega_{ref}}{2})t - \theta_c\Big]. \tag{8.1}$$

This would therefore result in the same beating signal as for the setup I have assembled, given by

$$V_{beat} = cos\Big[\omega_{ref}t + 2(\theta_c + \theta_f)\Big], \tag{8.2}$$

and the electronics would be arranged in the same way.

This geometry does not need a beam splitter that picks off the reflected beams. The only loss of optical power due to the cancellation system, then comes from the small fraction of light that is retro-reflected at the remote end of the fiber. For our purposes it is desirable to minimize the loss of optical power due to the cancellation system. This is an advantage with this alternative setup.

The setup in Figure 8.1 should also allow more light that has been twice through the fiber to reach the photodetector, compared to the setup that was assembled in this project. The AOM was set so that roughly 70% was diffracted into the +1st order, and 15% was left in the 0th order during my measurements. For the setup in Figure 8.1, the beam that has been retro-reflected through the fiber will pass the AOM, leaving 15 % of its power in the beam of interest that then reflects of the mirror to the photodetctor. For the setup assembled in this project, the beam that has been retro-reflected through the fiber will pass the AOM, leaving 70 % of its power in the beam of interest that then reflects of the 10% reflectivity beam splitter to the photodetector. In total 7% of the power out from the fiber in the backwards direction reaches the photodetector. This rough estimation shows that the power in this beam on the photodetector should be roughly doubled with the alternative setup. A higher ratio between light that has been twice through the fiber and the unwanted reflections can thus be obtained with this alternative setup. The unwanted reflections from the AOM may also decrease, because the reflection from the first facet of the AOM would not be reflected into the beam going to the photodetector.

The power in the beam on the photodetector that has not been through the fiber, should with the alternative setup be well above the power necessary for the system to work good, because the power in the beam going into the cancellation system can be set as high as 100 mW.

8.1 Slow Light Laser Locking

An extension of the previously used setup for laser locking to a slow light crystal cavity was assembled. This setup includes the fiber noise cancellation system and, also some minor additions, such as a motorized flip filter. Because an AWG was not functioning properly, no laser locking attempts were made, and how well this setup actually would work remains to be seen in future experiments.

Acknowledgements

First of all I would like to thank my supervisor Lars Rippe. I have had great time during this project and I feel like you have taught me lots of things that will be useful in my future career as an engineer. I would also like to thank the head of the group Stefan Kröll for the opportunity to do my master's project with the Quantum Information Group. Finally, I would like to thank the other members of the group Adam Kinos and Andreas Walther.

References

[1] Adam Wiman. *Laser stabilization to a low-expansion Fabry-Pérot cavity*. Master's thesis, Lund University, 2011.

[2] N. Hinkley et al. *An Atomic Clock with 10^{-18} Instability*. Science, **341**(6151):1215–1218, 2013.

[3] K. Predehl. *A 920 km Optical Fiber Link for Frequency Metrology at the 19th Decimal Place*. PhD thesis, Ludwig-Maximilians-Universitat Munchen, 2012.

[4] Theodor Strömberg. *Laser Stabilization using a Slow light Cavity*. Master's thesis, Lund University, 2015.

[5] Haifeng JIANG. *Development of ultra-stable laser sources and long-distance optical link via telecommunication networks*. PhD thesis, Université Paris, 2010.

[6] O. Terra et al. *Phase-coherent comparison of two optical frequency standards over 146 km using a telecommunication fiber link*. Applied Physics B-Lasers and Optics, **97**:541–551, 2009.

[7] Long-Sheng Ma, Peter Jungner, Jun Ye and John L.Hall. *Delivering the same optical frequency at two places: accurate cancellation of phase noise introduced by an optical fiber or other time-varying path*. OPTICS LETTERS, **19**(21), 1994.

[8] Lars Rippe. *Quantum computing with naturally trapped sub-nanometre-spaced ions*. PhD thesis, Lund University, 2006.

[9] Anders Rönnberg. *Fiber Noize Cancellation*. Master's thesis, Lund University, 2013.

[10] Seth M. Foreman. *Femtosecond Frequency Combs for Optical Clocks and Timing Transfer*. PhD thesis, University of Colorado, 2007.

[11] Tore Hägglund. *REGLERTEKNIK AK Föreläsningar*. Institutionen för Reglerteknik Lunds Tekniska Högskola, 2013.

[12] M.C.Teich B.E.A Saleh. *FUNDAMENTALS OF PHOTONICS Second Edition*. Wiley & Sons, Hoboken, New Jersey, 2007.

[13] N. Darkwah Oppong. *Cancelation of optical phase noise induced by an optical fiber*. ETH Zurich, 2015.

[14] J. Karlsson. *Cerium as a quantum state probe for rare-earth qubits in a crystal*. PhD thesis, Lund University, 2015.

[15] Eric D. Black. *An introduction to Pound-Drever-Hall laser frequency stabilization*. Am. J. Phys, **69**(1):79–87, 2001.

[16] John S. Toll. *Causality and the Dispersion relation:Logical Foundations*. PYSICAL REVIEW, **104**(6):1760–1770, 1956.

[17] M. Sabooni, Q. Li, L. Rippe, R. Krishna Mohan, and S. Kröll. *Spectral Engineering of Slow Light, Cavity Line Narrowing, and Pulse Compression*. Phys. Rev. Lett., **111**, 2013.

[18] Stanford Research Systems. *Operation and Service Manual Analog PID Controller SIM960*, 2013.

[19] Lars Rippe. Personal Communication, 2017.

[20] David W. Allan. *Statistics of Atomic Frequency Standards*. Proceedings of the IEEE, **54**(2):221–230, 1966.

[21] New Focus. *Operating Manual LB1005 High-Speed Servo Controller*, Revision 1.

[22] David B. Hume. *Two-Species Ion Arrays for Quantum Logic Spectroscopy and Entanglement Generation*. PhD thesis, University of Colorado, 2010.